Late Holocene climate development of Bjørnøya, Svalbard, based on chironomid analysis

Henriikka Kivilä

8.11.2014

Master's thesis

DEPARTMENT OF GEOSCIENCES AND GEOGRAPHY

UNIVERSITY OF HELSINKI

Tiedekunta/Osasto Fakultet/Sektion – Faculty	Laitos/Institution– Department
Faculty of Science	Department of Geosciences and geography

Tekijä/Författare – Author

Henriikka Kivilä

Työn nimi / Arbetets titel – Title

Late Holocene climate development of Bjørnøya, Svalbard, based on chironomid analysis

Oppiaine /Läroämne – Subject

Geology / Hydrogeology and environmental geology

Työn laji/Arbetets art – Level	Aika/Datum – Month and year	Sivumäärä/ Sidoantal – Number of pages
Master's thesis	11/2014	72

Tiivistelmä/Referat – Abstract

Recent climate related changes in the Arctic have risen concern and interest to better understand the mechamisms of arctic climate system and to predict the future reponse. Due to short instrumental monitoring a palaeoenvironmental view is required to reveal and understand long-term changes, yet high-resolution palaeoecological and -climatological studies are sparse. Bjørnøya, the Bear Island, (74°30' N, 19° E) is a key site for terrestrial palaeoclimate records along the heat transport system of the North Atlantic Current, with the possibility of linking records from northern Fennoscandia and Arctic Svalbard.

A summer temperature series for the past ca. 1000 years was reconstructed from a 64 cm surface sediment core from lake Ellasjøen, SW Bjørnøya, based on quantitative palaeoenvironmental modelling of subfossilized chironomid assemblages. Quality of reconstructions was assessed with modern analogue techique and principal component analysis. To support the interpretation and receive a more holistic view of the lake history, in-lake processes, catchment interaction and factors behind the changes, a multi-proxy approach was chosen. Sediment physical characteristics: water content, loss-on-ignition, magnetic susceptibility and spectrocolorimetric identification of sedimentary signatures and components, in addition to composition and diversity of the chironomid assemblage, were used to trace a comprehensive picture of past changes. Radiometric dating was conducted to assess the temporal context of the sedimentary series.

The results reveal that Ellasjøen is a climatically sensitive lake and preserves a history of substantial changes. A general pattern is detected where Medieval Warm Period features very modest warmth, followed by warming summer temperatures untill 1600 AD, when the temperature trend starts to decrease towards culmination of the Little Ice Age at 1740 AD. A warming trend ever since is persistent but does not exceed past warmth. Results suggest higher seasonality during Little Ice Age and seek to explain causes for modest recent warmth. Reconstructed climate development is in good agreement with recent results from surrounding areas and a complex set of ice-ocean-atmosphere interactions is proposed as driving factors. The findings of this study highlight the importance of regionally solved high-resolution climate records and tracing of seasonal climate components to fully understand the variation and interrelationship of driving factors affecting the Arctic climate dynamics in the eastern North Atlantic sector.

Avainsanat – Nyckelord – Keywords

late Holocene, arctic climate, Bjørnøya, Bear Island, palaeolimnology, chironomid analysis

Säilytyspaikka – Förvaringställe – Where deposited

University of Helsinki, Department of Geosciences and geography, Division of Geology

Muita tietoja – Övriga uppgifter – Additional information

Tiedekunta/Osasto Fakultet/Sektion – Faculty	Laitos/Institution– Department
Matemaattis-luonnontieteellinen tiedekunta	Geotieteiden ja maantieteen laitos

Tekijä/Författare – Author

Henriikka Kivilä

Työn nimi / Arbetets titel – Title

Huippuvuorten Karhusaaren ilmastokehitys myöhäis-holoseenissa chironomidianalyysiin perustuen

Oppiaine /Läroämne – Subject

Geologia / Hydrogeologia ja ympäristögeologia

Työn laji/Arbetets art – Level	Aika/Datum – Month and year	Sivumäärä/ Sidoantal – Number of pages
Pro gradu -tutkielma	11/2014	72

Tiivistelmä/Referat – Abstract

Viimeaikaiset ilmaston muutoksen vaikutukset pohjoisilla napa-alueilla ovat huolestettuvia, minkä vuoksi kiinnostus ilmastomekanismien parempaan ymmärtämiseen on lisääntynyt. Mittauslaitteiden kattama aika on napa-alueilla yleensä lyhyt, joten ilmastovasteiden tutkimisessa tarvittavat pitkät aikasarjat edellyttävät luonnon arkistojen hyödyntämistä. Tarkan resoluution tutkimukset ekologian ja ilmaston kehityksestä pohjoisilla alueilla ovat kuitenkin harvassa. Karhusaari (74°30'N, 19° E) on sijainniltaan avainasemassa ilmastotutkimuksen suhteen, sillä se tarjoaa ainutlaatuisen mahdollisuuden tutkia järvisedimenttisarjoja Pohjois-Atlantin merivirran välittömässä vaikutuspiirissä yhdistäen Pohjois-Norjan ja Huippuvuorten ilmastokehityksen mekanismit toisiinsa.

Karhusaaren Ellasjøen järvestä nostetusta 64 cm pitkästä pintasedimenttisarjasta rekonstruoitiin viimeksi kuluneen 1000 vuoden ajalta kesälämpötilaa hyödyntäen siirtofunktiomallinnuksen avulla subfossiilista surviaissääskilajistoa (Chironomidae). Tulosten hyvyyttä arvioitiin moderni analogia -tekniikalla ja pääkomponenttianalyysillä. Tulkinnan tueksi ja järven historian, valuma-alueprosessien ja taustatekijöiden ymmärtämiseksi hyödynnettiin usean muuttujan aineistoa. Sedimentin fysikaalisten ominaisuuksien, vesipitoisuuden, hehkutushäviön, magneettisen suskeptibiliteetin sekä spektrofotometrisen väri- ja komponenttianalyysin lisäksi surviaissääskipopulaation rakennetta ja monimuotoisuutta analysoitiin tilastollisin menetelmin rakennettaessa kokonaiskuvaa järven muutoshistoriasta. Ajoitukset tehtiin radiometrisin menetelmin.

Tutkimuksen tulokset osoittavat, että Ellasjøen on ilmastoherkkä järvi, jonka sedimentti-arkistoissa on säilynyt todisteita merkittävistä ympäristönmuutoksista. Yksinkertaistettuna tutkitun sarjan kehitys osoittaa, että Keskiajan lämpimänä kautena olosuhteet olivat vain hieman nykyistä lämpimämmät ja että niitä seurasi lämpenevä trendi aina 1600 -luvun taitteeseen asti. Sen jälkeen kesälämpötila laski kohti Pienen Jääkauden huipentumaa 1740 AD. Tämän jälkeen kesälämpötila on ollut selkeässä nousussa aina nykypäiviin asti, kuitenkaan ylittämättä edeltävien ajanjaksojen keskilämpötiloja. Tuloksista voidaan päätellä, että vuodenaikaisvaihtelut olivat hyvin suuria Pienen Jääkauden aikana, ja niistä on etsittävissä syitä viimeaikaiseen suhteellisen vähäiseen lämpenemiseen. Tulokset sopivat yhteen lähialueilta julkaistun aineiston kanssa ja viittaavat monimutkaisiin ilmakehän, valtameren ja merijään välisiin prosesseihin taustatekijöinä. Tutkimuksen tulokset korostavat paikallisten tarkan resoluution ilmastosarjojen ja kausiluontoisuuden huomioimisen tärkeyttä pyrittäessä saavuttamaan parempi käsitys arktisen ilmaston taustatekijöistä, niiden vaihteluista ja yhteyksistä toisiinsa Pohjois-Atlantin arktisilla alueilla.

Avainsanat – Nyckelord – Keywords

myöhäis-holoseeni, arktinen ilmasto, Karhusaari, paleolimnologia, chironomidianalyysi

Säilytyspaikka – Förvaringställe – Where deposited

Helsingin yliopisto, Geotieteiden ja maantieteen laitos, Geologian osasto

Muita tietoja – Övriga uppgifter – Additional information

CONTENTS

Cover picture: Glimpse of sun in the receding fog, view towards west over Ellasjøen, Bjørnøya July 2013.

1. INTRODUCTION

1.1. Sedimentary research and chironomids as tools for climate studies

Lake sediments are known to be valuable archives of palaeoenvironmental information, commonly providing a continuous record with potential to temporal high resolution. Lake environments are subject to various natural and human induced in-lake processes and changes within the catchment area, effects of which are unified in the lake sediment (e.g. Cohen 2003, Battarbee et al. 2012). Differentiating the response of a single variable is often challenging, hence a multi-proxy approach, where information on several physical, chemical or biological records are used to support the final interpretation, is preferred (Birks and Birks 2006).

Subfossil remains of non-biting midge i.e. chironomid larvae (Diptera: Chironomidae) provide an efficient tool for palaeoecological studies (Brooks and Birks 2001, Walker 2001, Brooks 2006). The family Chironomidae is extremely rich in species, distributed on a large geographical gradient and adapted to various ecological conditions, widely populating aquatic and terrestrial environments (Armitage et al. 1995). As an outcome chironomid remains often are abundant in lacustrine sediments also in demanding conditions where many other bio-indicators cannot survive, such as polar lakes.

The chironomid populations respond sensitively to various environmental factors, including changes in temperature, pH, oxygen level, trophic status, lake level and food-webs (Walker 2001). The palaeoenvironmental indicator potential has been discovered long ago (Andersen 1938, Stahl 1969, Hofmann 1988) but chironomid analysis didn't become common until the 1990's encouraged by building of large modern training sets (Walker 2001), which allows assessing of quantitative reconstruction of palaeoassemblages based on modern series. However, during the past few decades a great rise in interest for studying palaeoecology and climatic change from down-core profiles has taken place (Birks et al. 2010). Chironomids have been used as indicators of for example hypolimnetic oxygen (Quinlan and Smol 2001a) and eutrophication (Brodersen and Quinlan 2006, Langdon et al. 2006), total phosphorus (Brooks et al. 2001) and lake level fluctuations (Kurek and Cwynar 2009), but are especially

recognized as a powerful proxy for quantifying past climate change, with emphasis on temperature development, in the northern hemisphere specifically mean July air temperature (Walker et al. 1991, Eggermont and Heiri 2012). In the Arctic context, chironomids are one of the few proxies available for summer temperature reconstructions and are known to respond to environmental change with promising results (e.g. Walker and Cwynar 2006, Luoto et al. 2011, Self et al. 2011, Axford et al. 2013).

Paradoxically the connection between temperature and chironomid response remains unsolved, but is most likely a combination of direct physical control on various life stages and indirect effect of climate on various environmental in-lake variables, such as chemistry, productivity and amount of nutrients (Eggermont and Heiri 2012). Furthermore, the effect of surface water rather than air temperature has been shown to be more important to all immature stages affecting the hatching, larval and pupal development, but air temperature, being strongly coupled with the surface water temperature, affects also adult midges and thus their reproductive behaviour (Eggermont and Heiri 2012 and references therein). Hence the air temperature reconstructions rely on the strong relationship between air and surface water temperatures, even if the latter is more relevant to chironomid development, but are also easier to validate in the presence of instrumental records.

1.2. Bjørnøya as a target for climate studies

The recent Arctic climate development has caused much concern, as the effects of the ongoing climatic change are amplified in the Arctic due to several positive feedback mechanisms (ACIA 2004, Serreze and Francis 2006). The understanding of natural ecological variability in the Arctic is hampered by lack of long-term monitoring (Quinlan et al. 2005), thus ecosystem responses to environmental change remain poorly understood.

The instrumental temperature record on Svalbard reaches back to 1911 (the homogenized Longyearbyen-Svalbard airport data series) while on Bjørnøya continuous measurements are obtained since 1920. A challenge for the instrumental measurements

in Svalbard is that temperatures can vary remarkably on daily, monthly and annual scales (Førland and Hanssen-Bauer 2003). Because of the seasonal differences, the annual mean temperature is generally reflecting more the fluctuations of the winter rather than summer temperature.

In larger climatic perspective the location of Bjørnøya is interesting, as it is located on the fluctuation area of the Arctic Front. It is the only land area in western Barents Sea in proximity to the division point of the northern and eastern branch of the North Atlantic Current, and within the influence area of East Spitsbergen and Bear Island Currents transporting cold polar waters from the north and east, thus it may provide climatic key information on the interaction of different water masses. The location may also allow shedding light to the linkage between the Arctic and northern Fennoscandia in a climatic and ecological context.

Previous palaeoecological and -climatological studies from the lakes on Bjørnøya are sparse. Pollen record for several lakes, including Ellasjøen have been studied (Hyvärinen 1968, 1970) and a multi-proxy study was carried out by Wohlfarth et al. (1995) who investigated a more northern lake Stevatnet. These studies concentrate on the deglaciation and early Holocene, with little interest on late Holocene. However, Wohlfarth et al. (1995) found the diversity of macrofossils high and reports chironomid remains common throughout the sediment series showing the high potential of chironomid analysis on lakes of Bjørnøya.

Ecosystem and surface sediment of lake Ellasjøen have recently been studied for pollution and organic contaminants (Evenset et al. 2004, 2005, 2007a, 2007b). A markedly important factor on the chemistry and ecology of Ellasjøen is strong bird influence. Evenset et al. (2007b) describes a sedimentation rate of 0.7 mm/year at lake Ellasjøen, which in the context of Arctic lakes is very high, thus denoting the potential for high-resolution sedimentary records.

1.3. Study objectives and hypothesis

The overall aim of this study is to reconstruct Late Holocene climate development from lake Ellasjøen, Bjørnøya by using biological and sediment physical proxies. Paleolimnological methods used are quantitative paleoenvironmental modelling based on chironomid assemblages and supportive physical methods, such as Loss-on-ignition (LOI) and spectrocolorimetry.

The principal hypotheses of this study is that the Late Holocene climate variability has affected lake Ellasjøen and its catchment area, and that these changes are preserved in the sediment record as changes in the biological and physical properties. The sediment archives of this isolated and pristine lake are expected to reflect the natural variability as very little anthropogenic disturbances occur.

The results are expected to reveal recent climatic development of previously unstudied area, improve understanding of late Holocene climate variability in the Arctic and contribute to discussion on on-going climate changes in the Arctic (see e.g. Masson-Delmotte et al. 2013). Every palaeoclimate record from Svalbard is unique and valuable, as especially summer temperature reconstructions from Svalbard and European Arctic are sparse (see Velle et al. 2011, D'Andrea et al. 2012). Hence, the need for high-resolution climate records is immense to understand the development on this Arctic sector, connected to the powerful heat transport mechanisms of the Atlantic Ocean.

2. STUDY AREA

2.1. Bjørnøya - geological and climatic setting

Bjørnøya, The Bear Island, is a small, isolated island in the European Arctic and the southernmost island of Svalbard archipelago. It is located at 74,33 - 74,52° N and 18,74 - 19,27° E, approximately midway from northern Norway to Spitsbergen (Fig. 1.). By size it is 20 km from north to south and 15 km west to east with a surface area of 178 km^2.

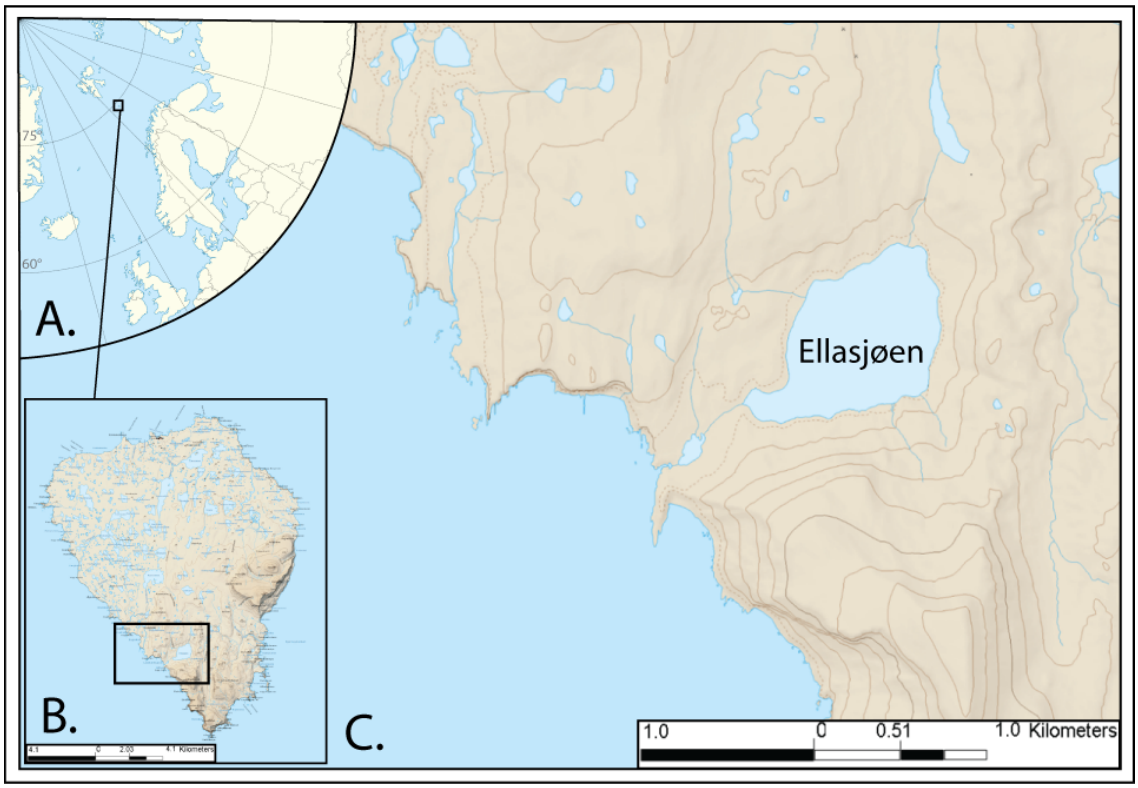

Figure 1. A) The location of Bjørnøya in the European Arctic. B) Map of Bjørnøya with the study area defined in SW. C) The study site: lake Ellasjøen and surroundings. Maps by Norwegian Polar Institute.

The maritime arctic climate on Bjørnøya is milder than in the rest of Svalbard. It is regulated by the Norwegian Current bringing warmth from the south and the East Spitsbergen current transporting cold from the north. The average yearly mean temperature on Bjørnøya was -2.4 °C during the calculation period of 1961–1990 (eKlima 2014). During the same time interval average temperature of the coldest month

was -8.1 °C (January) and the warmest months 4.4 °C (July-August). Overall the instrumental data demonstrates a fairly constant temperature history for the past 100 years as seen in Figure 2. However, a persistent warming trend can be seen especially in the mid-winter temperatures during the past 10 years. The instrumental period reaches back to 1920 and the Bjørnøya temperature series is considered homogeneous despite relocation of the meteorological station in 1945 (Nordli et al. 1996). Until 1941 the station was located in Tunheim, on the eastern coast. During the Second World War (1941–1945) no measurements were carried out, and after the war station was established to the present location on the north coast.

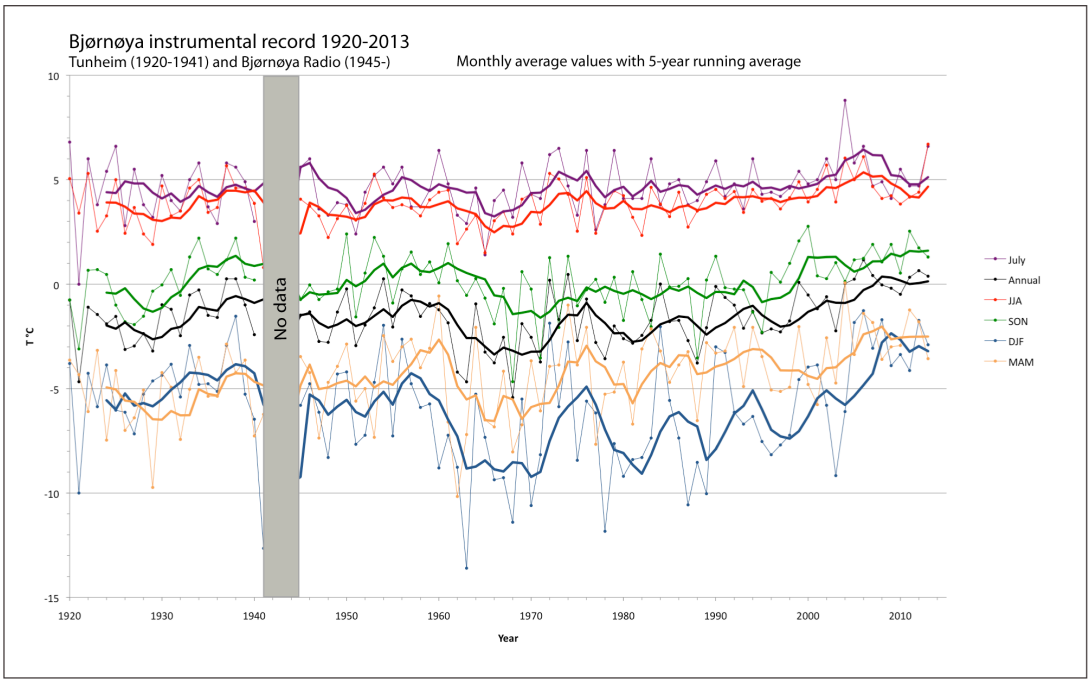

Figure 2. The instrumental air temperature data from Bjørnøya reaching back to 1920, divided into seasonal clusters: June-July-August (JJA), September-October-November (SON), December-January-February (DJF) and March-April-May (MAM). Also mean annual temperature and mean July temperature are displayed. No data is available from 1941–1945 due to the Second World War.

Compared to the data from Longyearbyen-Svalbard airport series (eKlima 2014), the seasonality is lower on Bjørnøya, with generally milder winters and cooler summers. However, seasonal temperature trends are in good agreement. The precipitation is considerably higher than on Spitsbergen with annual mean precipitation of 371 mm during the observation period of 1961–1990. Approximately 60 % of annual

precipitation falls as snow. During summer months the island is frequently covered in dense fog.

Geographically Bjørnøya is divided into two different parts: mountainous southern part and northern plains (eg. Horn and Orvin 1928, Salvigsen and Slettemark 1995, Wohlfarth et al. 1995, Worsley et al. 2001). The southern mountains reach up to 536 meters, Urd of Miseryfjellet being the highest peak (Horn and Orvin 1928). The northern part is low-lying, mainly less than 40 meters above sea level and very flat, typifying a large strandflat (Nansen 1922), a common feature along the coasts of Svalbard. Another distinct feature are the prominent shore cliffs, seawards Bjørnøya terminates to steep bedrock cliffs of 10–400 meters and low-lying shoreline is rare (Hjelle 1993). The cliffs are wave cut and since there is no shelter from the action of the ocean erosion rates are high.

Bjørnøya sits on the border of the North Atlantic Ocean and the Barents Sea, close to the edge of continental shelf. It is located on an elevated landform of Stappen high composing of Late Paleozoic deposits (Gabrielsen et al. 1990). Bedrock on the island is of same origin and comprises to a very large portion of Devonian to Triassic sedimentary succession (Horn and Orvin 1928, Worsley and Edwards 1976). Proterozoic deposits and Ordovician carbonates are present at the southern mountains. The Devonian-Triassic succession features carbonates, sand- and siltstones with coal bearing horizons. In the limestone areas karst features are common, such as dolines, caves, subsurface drainage channels and collapsed karst landforms (Salvigsen and Slettemark 1995).

The Quaternary sediments on the island are thin and discontinuous (Salvigsen and Slettemark 1995). Wide areas of the island consisting of sandstone bedrock are covered by autochtonous block fields. Thin layers of cryoturbated glacial tills are exposed on the coastal cliffs, typically on top of polished bedrock surface. Soil formation on the island is tenuous. The permafrost is estimated to reach 60-70 m depth and the thickness of active layer to be 0.75 m (Horn and Orvin 1928). Permafrost features are widespread on the island and markedly common in the limestone terrain (Wohlfarth et al. 1995).

Salvigsen and Slettemark (1995) state that only small scale local glaciations have existed during the Late Weichselian, based on the glacial striae direction and local origin of all displaced material. No deposits of marine origin or raised beaches are found on the island, hence Bjørnøya is considered not to have been overridden in large scale by the Barents Sea Ice sheet during the last glaciation but only been covered by non-erosive, thin glaciers. Bjørnøya is surrounded by deep troughs, Storfjordrenna on the north side and the massive Bjørnøyrenna in the south. These troughs, especially Bjørnøyrenna, served as the major drainage channels for the Barents Sea Ice sheet during the past deglaciations (Landvik et al. 1998).

Deglaciation time of the lowlands on Bjørnøya is estimated to approximately 10 000 (11 500 cal BP) years ago, as the sedimentation in the lakes started around that time (Hyvärinen 1968, Wohlfarth et al. 1995). Peat deposits on the southern mountains indicate deglaciation of the higher areas before 8700 BP (9850 cal BP) (Salvigsen and Slettemark 1995).

The hydrological system on Bjørnøya comprises hundreds of lakes and ponds, most being small and remarkably shallow (Wohlfarth et al. 1995). Lake basins are created by glacial carving reaching only a few meters depth and many of the water bodies dry out during summer (Salvigsen and Slettemark 1995).

2.2. Lake Ellasjøen and the catchment area

The study site, lake Ellasjøen (74°23'N, 19°01'E), is situated in the southwestern part of Bjørnøya (Fig. 1.). Amongst the numerous small and shallow lakes on the island Ellasjøen is an exception. Located in the mountainous southern part of the island, lake Ellasjøen is surrounded by steep reliefs on two sides, with Alfredjellet (421 m) to the south and limestone cliffs reaching up to 156 m on the eastern side (Norwegian Polar Institute 1992). The terrain north of Ellasjøen is of low relief, gently sloping towards the lake but further out rising up to 163 meters on Oswaldfjellet. The mountainous southern part of Bjørnøya receives more precipitation than northern areas. Measurements at Ellasjøen show a precipitation rate (rain and condensed fog) of 3.15 times higher than at the meteorological station (Evenset et al. 2007a).

2.2.1. Geological setting and catchment area

Bedrock where lake Ellasjøen lies is composed of two different types (Fig. 3.). The eastern side of the lake displays Middle to Late Ordovician (472–443 Ma after Cohen et al. (2013)) carbonate rocks which are part of the Hecla Hoek -basement complex also found elsewhere in Svalbard, correlation first suggested by A. E. Nordenskiöld in 1864 (e.g. Horn and Orvin 1928, Worsley et al. 2001). This Ymerdalen formation composes of black or dark grey dolomites in the lower part and fossilferous limestone (Holtedahl 1920) of the same colour in the upper part. Both members lie within the catchment area while only lower dolomites are present in the lake basin (Norwegian Polar Institute 1996). There is a normal fault line of SE-NW orientation in the Ordovician strata at the lake site (Fig. 3.), which is a common feature in the Hecla Hoek of Bjørnøya (Worsley et al. 2001).

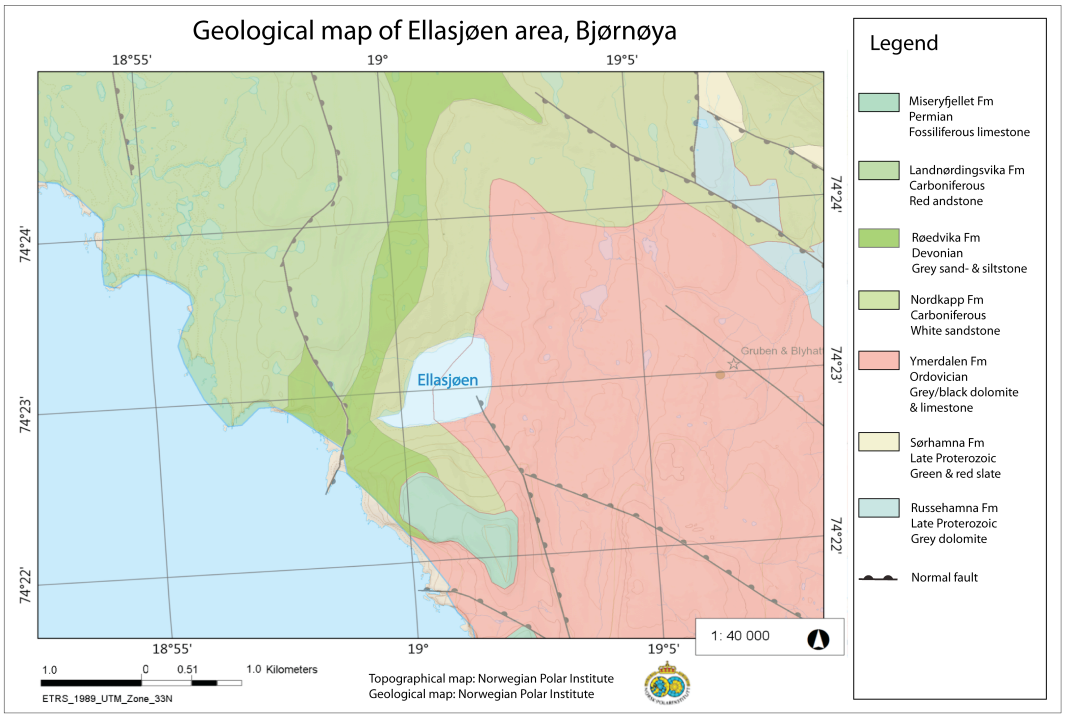

Figure 3. Bedrock and geological features in the surroundings of lake Ellasjøen.

The western side of lake Ellasjøen features oldest parts of the Late Palaeozoic sedimentary succession dominant on Bjørnøya. Upper Devonian strata rests on top of the Hecla Hoek basement separated by a distinct, angular unconformity (Horn and

Orvin 1928). Around the lake the strata belongs to Røedvika Formation of Famennian age, 372–359 Ma according to Cohen et al. (2013), and composes of a succession of coalbearing flood plain deposits and sandstones. In literature Røedvika Formation is often referred to as 'Ursa-sandstone' (eg. Horn and Orvin 1928, Wohlfarth et al. 1995, Worsley et al. 2001). On the catchment area also Lower to Middle Carboniferous strata following continuously Røedvika Formation is displayed. These Nordkapp and Landnørdingsvika Formations feature a succession of non-marine sandstones and conglomerates, white by colour in Nordkapp Formation and distinct red in Landnørdingsvika Formation (Worsley et al. 2001).

Around the lake bedrock is widely exposed and Quaternary features form only a thin layer on the surface, if any (Fig. 4.). Evidence of past glaciations is certain. The terrain is strongly controlled by bedrock, and areas featuring sandstones are typically covered with *in situ* block fields, especially north of Ellasjøen. On the north side a row of small, elongated incisions in bedrock, possibly formed by glacial or glaciofluvial carving, descend towards the lake. On the bottom of the incisions some fine-grained sediment occurs, plausibly deposited in seasonal standing water. Bedrock outcrops on the ridges in between and the area is vastly covered in in-situ weathered sandstone blocks. On the block fields some boulders sit on top of each other giving a clear proof of past glaciations (Fig. 5.). Lithologies of blocks are consistently of the underlying bedrock an during fieldwork only one cobble of exotic lithology was found north of Ellasjøen, featuring red sandstone likely of Landnørdingsvika Formation and thus indicating transport from NW. Only vegetation in this terrain composes of mosses, which can form strikingly thick mats. Some higher plants can occur in flat areas with fine-grained sediments.

On the south side terrain is dominated by sandstone blocks featuring also rock fall from cliffs of Alfredfjellet and rapid mass movement deposits. Closer to the shoreline the blocks get fewer and thin mineral soil with grassy vegetation dominates. There is patchy evidence of paleoshorelines. The terrain close to the border to carbonate bedrock is blocky all the way down to the shoreline and may feature old mass movements.

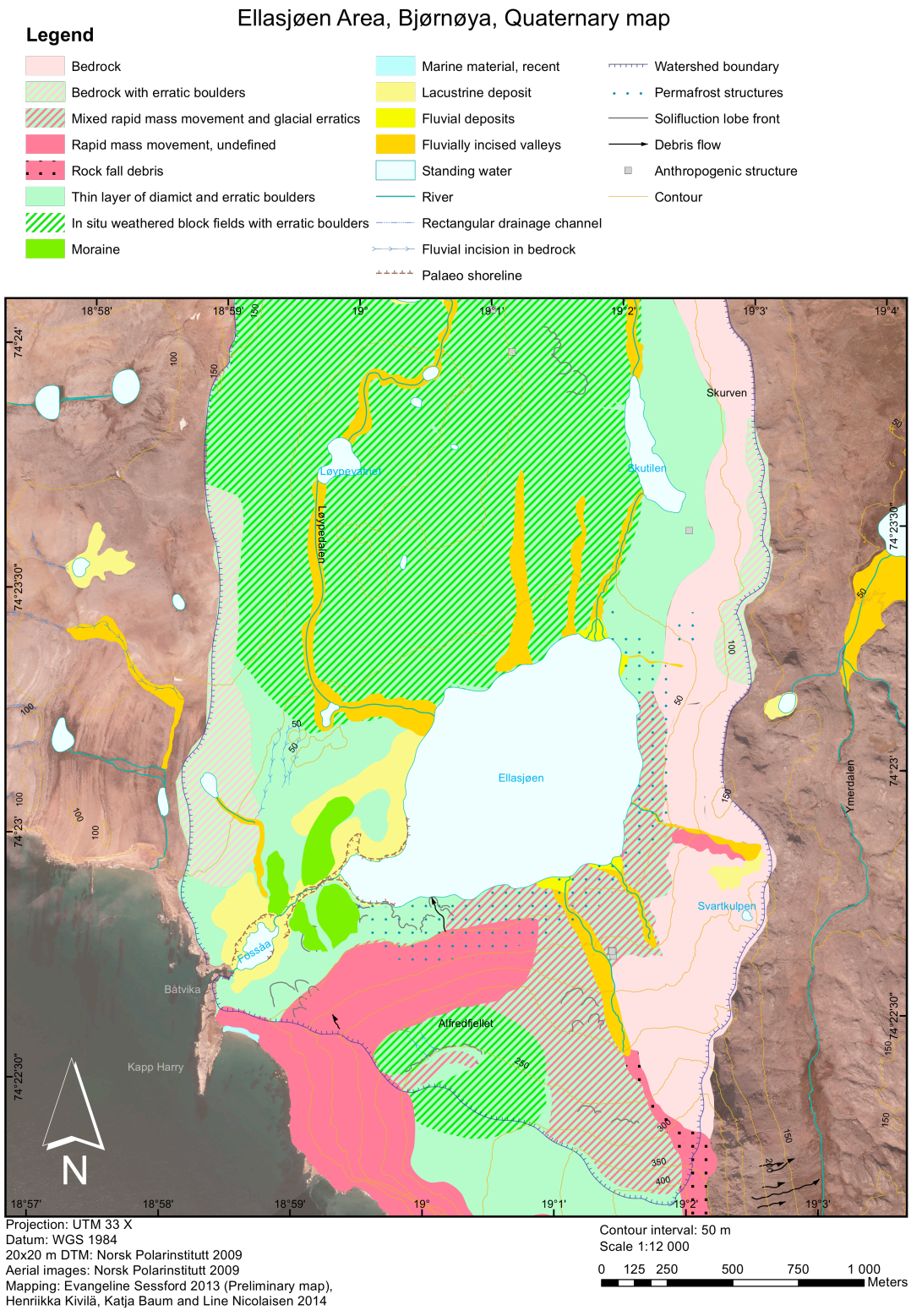

Figure 4.The Quaternary features mapped at the catchment area of lake Ellasjøen. The catchment is dominated by bedrock exposure and varying glacial evidence. In the southwestern part glacial deposits give a clear indicator of glacial activity, but scattered erratic boulders are found through the whole area.

The eastern side of the lake in the carbonate country features mainly bedrock exposure. The cliffs are barren and closer to Ellasjøen thin mineral soil is present sporadically (Fig. 5.). Solifluction is well-developed and thin moss layers cover level surfaces. The terrain on lower slopes features small ridges or 'steps' that seem like solifluction lobes or even palaeo shorelines from far apart, however this feature is purely driven by the bedrock construction. Two abandoned channels, which might still serve as snowmelt channels can be seen on the hillsides.

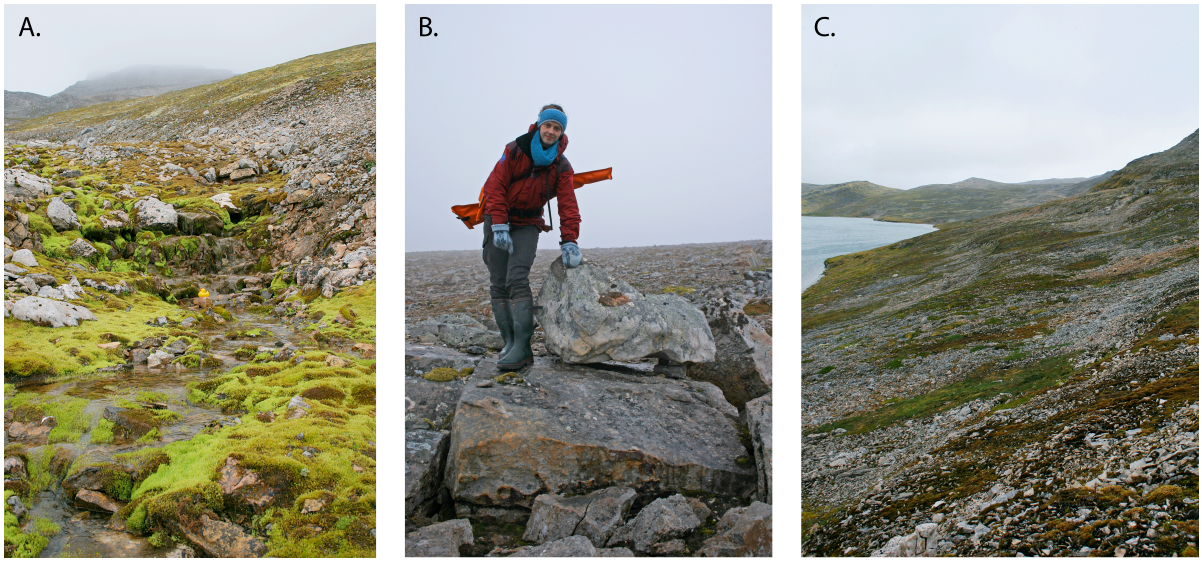

Figure 5. A. One of the larger inflows of Ellasjøen, representing the small fluvial input at present. B. Erratic on top of another boulder in the well-weathered northern block fields, Katja Baum for scale. C. Cryoturbated and soliflucted thin mineral soil east of Ellasjøen. Northern shore with incised valleys on the background.

On the western side of the lake sandstone territory does not feature block fields but tight diamictic sedimentary deposits of glacial origin and varying thickness, with alternating vegetation and scattered erratic boulders. Two moraines were mapped west of the lake (Fig.4.). The moraines consist of diamicton and boulders on the moraines consist partially of local Nordkapp formation, partially of Røedvika formation. In the coastal cliff exposures of Landnørdingsvika, Båtvika and Hamnevika the thickness of these diamictic deposits varies from almost nothing up to a couple of meters, displaying

relatively coarse material and large blocks within the matrix. Salvigsen and Slettemark (1995) document discontinuous deposits exposed on coastal cliffs as till.
Weathering on the study area is extremely intense and is very visible on the barren block fields. This directs interpretation towards cold-based ice cover in the past. Although, in the moist climate of Bjørnøya weathering rates higher than in most arctic regions can be expected. Soil formation on the area is tenuous and some thin fine-grained mineral deposits that could be referred as soil are associated with permafrost and periglacial processes.

2.2.2. The lake and the drainage system

Lake Ellasjøen is situated 20.8 m above sea level (Horn and Orvin 1928, Hyvärinen 1968) and has an area of 0.73 km^2. A retention time of 1.5 years has been estimated (Evenset et al. 2004, 2005). Ellasjøen is a deep lake with reported maximum depth ranging from 43 m (Horn and Orvin 1928) to 34 m (Evenset et al. 2004, 2007b). In this study the deepest measurement is obtained at 31 m. Horn and Orvin (1928) states the basin of Ellasjøen to be widely around 30 m depth. Whereas the average depth in lakes of Bjørnøya is only a few meters, source for the depth of Ellasjøen has been a matter of discussion. According to Horn and Orvin (1928) it was Nathorst (1899) who first suggested the lake owing its depth to dislocations as there is a fault line running through the lake. Horn and Orvin (1928) argue for a glacial abrasive impact, intensity following the changes in bedrock and its resistivity to erosion.

The ice-free period on Ellasjøen lasts from June to mid-November (Evenset et al. 2004). Aquatic vegetation consist primarily of submerged mosses as higher plants have not been observed from Ellasjøen (Engelskjøn 1986). Documented water temperatures range between 5.1 and 7.4 °C on July 16th to August 22nd in 1978 (Klemetsen et al. 1985). These observations indicate no summer stratification and merely tenuous thermal gradient between the surface and bottom waters. The lake is exposed to strong westerly winds contributing to the mixing of waters.

As reported by Klemetsen et al. (1985) the water is also slightly alkaline, pH ranging from 7.3 to 7.6, and the Secchi-depth is only 3.5 m. The lake water is turbid greyish-

greenish in colour with low transparency due to green algae. The appearance is typical to a lake with strong bird influence, not surprisingly as surroundings of Ellasjøen are teeming with seabirds. A colony of little auks (*Alle alle*) nest on the cliffs of Alfredfjellet and large flocks of kittiwake (*Rissa tridactyla*) accompanied by smaller numbers of glaucous gulls (*Larus hyperboreus*) use the lake as a resting and bathing place. According to the Norwegian Polar Institute bird surveys up to 20 000 birds visit the lake during one day. As a result of high bird influence Ellasjøen has relatively high productivity for an arctic lake (Evenset et al. 2007b).

The drainage system and watershed of Ellasjøen are fairly easily definable, in contrast to many other lakes on Bjørnøya. The only outflow from the lake drains towards west/ south-west to the small shallow lake of Fossåa before reaching the ocean in Båtvika (Fig. 6.). Inflows on the other hand are several. The two lakes Skutilen and Løypevatnet drain to Ellasjøen both from the north. At the time of field investigations the inflow from Løypevatnet was negligible. The drainage channel was still well developed showing signs of recent water flow. Though, the thick moss layer on blocks and boulders would suggest that no large quantities of water drain in these channels at present.

Drainage from Skutilen runs through a channel cut into the bedrock following the border of sandstone and limestone. This inflow contains more water and upstream appears as a lively creek. The water gets less as Ellasjøen is approached, presumably due to water disappearing in underground cracks associated with bedrock seam. On the shore of Ellasjøen a relatively large, nowadays inactive delta formation indicates considerably higher discharge from Skutilen in the past.

The main drainage reaching lake Ellasjøen on the surface comes from the south/south-east via two streams running on both sides of the Norwegian Polar Institute bird watching station (Figures 5. and 6.). Both streams are cutting into the limestone bedrock, the western one running in the seam of carbonates and sandstone. Both streams have a palaeodelta close to the present lake level. At the time of observations the eastern drainage channel had the most water but the considerably higher level of

incision and larger size of the palaeodelta suggest the western drainage to have been greater or longer lived in the past.

On the southern side of the lake there is no other major drainage but on the low-relief slopes between the lake and the sandstone cliffs small-scale surface flow is common. It has a tendency to form small, complex channels, which dry out or disappear underground just to show up again a few meters away. A plausible source for the water is thawing permafrost. Furthermore, the crack and fault systems can serve as pathways for underground inflow, albeit this can be considered marginal due to permafrost.

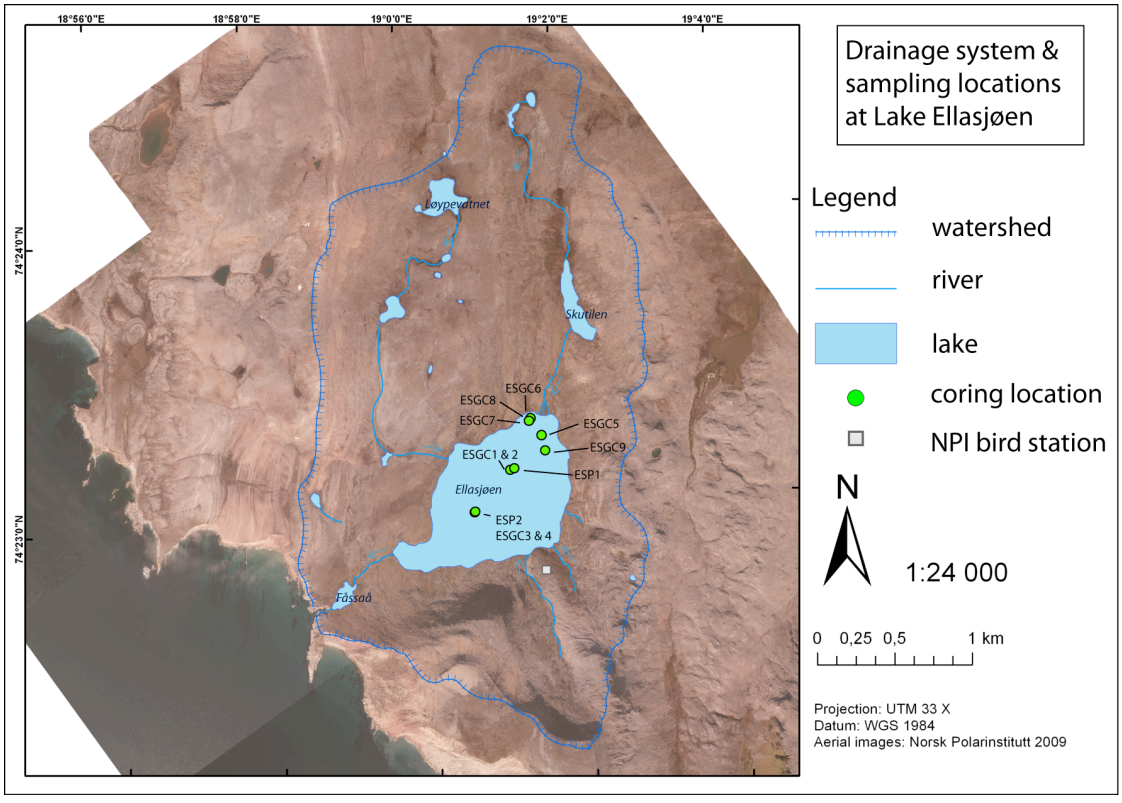

Figure 6. The drainage system and coring locations of lake Ellasjøen. ESP1 and 2 refer to two long piston cores and ESGC1–9 to nine surface gravity cores.

3. MATERIALS

3.1. Field work, sampling and mapping

Fieldwork on Bjørnøya was carried out as a one-week field campaign on 21.7.–27.7.2013. Lake sediment sampling was performed from a three-point anchored steel platform stabilized on top of two inflatable rubber boats (Fig. 7). For long cores a Nesje-type piston percussion corer (Nesje 1992) was used. Surface sediments and water-sediment interfaces were retrieved with an UWITEC gravity corer reinforced with a small hammering device (UWITEC Ltd., Austria). During the field period 2 approximately 6 meters long piston cores were obtained along with 9 short surface cores. The long cores ESP1-13 and ESP2-13 (Fig. 6.) were taken from the deeper part of the lake basin, with water depths of 31 m and 28 m respectively (Table 1.). Two surface cores were taken at the proximity of each piston core location to complete the long core with undisturbed surface sediments. ESGC1-13 and ESGC2-13 accompanying ESP1-13 were retrieved from 29,5 m water depth, correspondingly ESGC3-13 and ESGC4-13 supplementing ESP2 were obtained from the depth of 26,8 m. The rest of the surface samples were collected from different depth zones of the lake, shown in Figure 6. All coreing and sampling data is displayed in Table 1.

Table 1. Name, core type and length, coordinate location and lake depth at each sampling location at lake Ellasjøen.

Core ID	Longitude E	Latitude N	Water depth (m)	Core length (cm)	Core type
ESGC1	19.01883602	74.38548502	29.5	64	UWITEC Gravity core
ESGC2	19.01883602	74.38548502	29.5	53	UWITEC Gravity core
ESGC3	19.01062704	74.38316298	26.8	91	UWITEC Gravity core
ESGC4	19.01062704	74.38316298	26.8	61	UWITEC Gravity core
ESGC5	19.02599802	74.38736801	13.5	34	UWITEC Gravity core
ESGC6	19.02393297	74.38838800	3.2	37	UWITEC Gravity core
ESGC7	19.02353098	74.38826102	9	46	UWITEC Gravity core
ESGC8	19.02352503	74.38823503	7	38	UWITEC Gravity core
ESGC9	19.02659498	74.38647098	19	51	UWITEC Gravity core
ESP1	19.01976398	74.38555601	31	580	Nesje Piston core
ESP2	19.01071102	74.38319399	28	565	Nesje Piston core

Prior to sampling ground penetrating radar (GPR) was run on the lake surface to determine basin topography and deepest areas. The GPR set up composed of Malå ProEx central unit accompanied with a 100 MHz rough terrain antenna. Data was collected with a rubber boat by pulling the antenna behind it. The antenna was sealed into a carefully capped PVC-tube to make it float and protect it from moisture (Fig. 7.).

The surroundings of the lake were briefly explored for bedrock and Quaternary features during the field campaign. The mapping is based on high-resolution aerial photographs and topographical maps provided by the Norwegian Polar Institute complemented with the field observations.

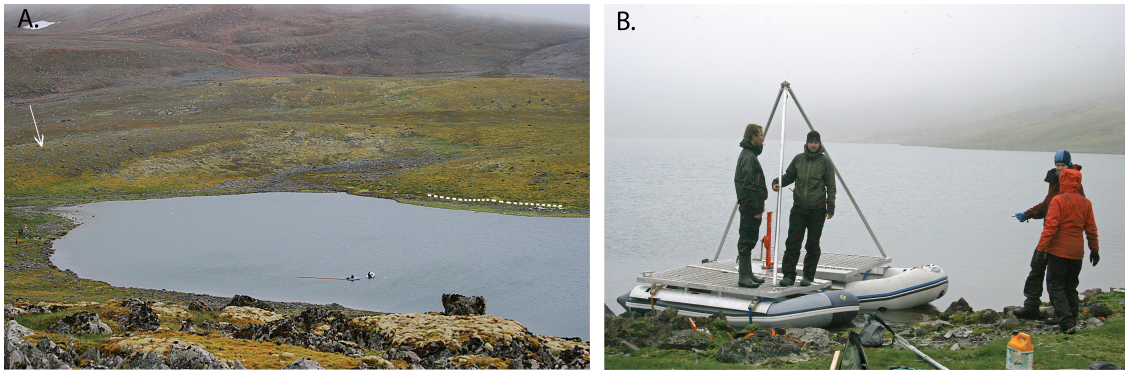

Figure 7. A. GPR measurements run on the lake. On the background larger of the mapped moraine ridges (arrow) and a paleoshoreline (below dashed line) can be seen, view towards NW. B. Coring platform and crew getting ready to drive into the mist to collect samples.

3.2. Samples and sample preparation

The nine short cores were photographed and briefly described at site. Top 10 cm of each core was sub sampled with an UWITEC compatible sub sampling set up. The surface sediments were sliced with a 0,5 cm interval and packed to plastic zip lock bags. Plant macrofossils discovered during sub sampling were picked out and stored in separate zip lock bags for AMS radiocarbon dating. Exceptions to this procedure are ESGC3-13 and ESGC7-13, which were preserved as a whole to provide a continuous record of the top

sediments and ESGC9-13, which was sub sampled only for top 5 cm due to limited time. The Nesje cores were cut into approximately 1 m sections on shore, capped and packed for transport and further analysis.

In the UNIS laboratory all the short cores were split 5.8.2013. Plastic tubes were cut with a circular saw and sediment was split with wire from top to bottom. All cores feature finely laminated grey-brown and black lake sediment widely in anoxic state. Cores ESGC5-13 and ESGC9-13 show dipping layers in some parts, indicating deltaic influence in the past. The split cores were well wrapped in plastic and stored in a cool room. The surface sediments sub sampled in the field were weighed and stored in a refrigerator.

Spectrocolorimetry and magnetic susceptibility were mesured on all split cores covered with a plastic film. For chironomid studies, loss-on-ignition and water content, the core ESGC1-13 was sub sampled with 1 cm interval. Plant macrofossil were picked from the split core and during sub sampling of ESGC1-13 in addition to those already collected in the field for dating purposes. All macrofossils were transferred to separate glass vials with distilled water and a drop of 10 % HCl to increase preservation prior to sending them for AMS radiocarbon dating.

3.3 Core ESGC1-13

For this study the core ESGC1-13 was studied in detail for chironomid analysis and physical proxies (loss-on-ignition, water content, magnetic susceptibility and spectrocolorimetry). ESGC1-13 is a 64 cm long gravity core obtained from a depth of 29.5 m (Table 1.). As retrieved the sediment appeared dark grey or black in color indicating anoxic state, except for the topmost 1,5 cm which featured an orange-brown horizon with oxidized iron. The well-preserved water-sediment interface was barren of all life visible to bare eye.

The split core displayed finely laminated, undisturbed lacustrine sediments as seen in Figure 8. The laminae are mostly of sub-millimetre scale and may present annual sedimentation patterns. The colour of the fresh sediment is in shades of brown tinted

towards red rather than olive. However, as the sediment quickly oxidizes after splitting causing colour change, the fresh surface colour was impossible to determine to detail. Large parts of the core are black or very dark but between 23 cm and 37 cm an area of lighter, brown sediments is evident. Another prominent red-brown layer at 51.5–53 cm depth appears very homogenous.

Four thin, dense, white layers are observed at 26.5-27 cm, 30 cm, 49.5 cm and 54 cm. White layers are present in all the gravity cores, serving as important marker horizons for core correlation. At 43.5 cm there is a layer very rich in moss remains. Throughout the core grain sizes remain small, mainly clay and silt fraction with little fluctuation. Some considerably larger grains can be found in the lighter coloured sediment intervals, one can be seen in the picture at 33 cm as a white spot (upper half). The lowermost part of the core below 52 cm appears slightly denser than the rest. In over all appearance the sediment material seems to feature continous and undisturbed, relatively homogenous sedimentation and high organic content, in the context of an arctic lake.

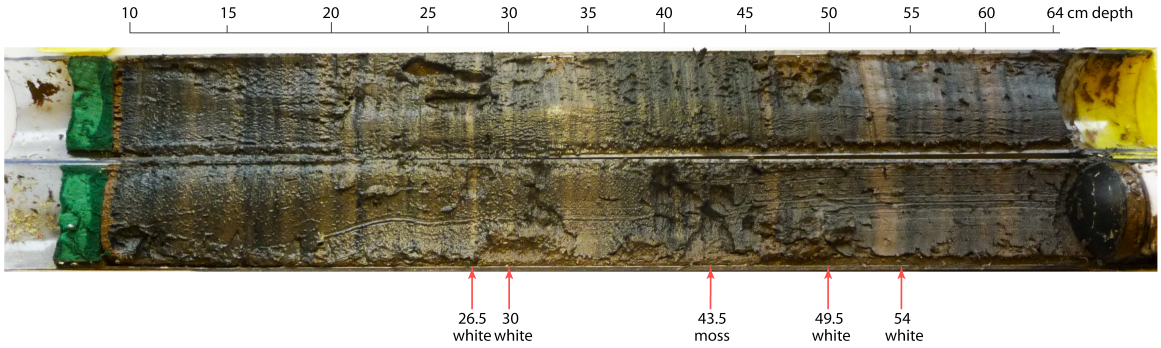

Figure 8. The appearance of gravity core ESGC1 immediately after splitting with dark finely laminated anoxic sediment. White marker horizons and a layer distinctly rich in plant macrofossils are marked. Scale is adjusted to the photographing angle. Uppermost 10 cm was sub sampled in the field and is not presented.

4. METHODS

4.1. Physical methods

4.1.1. Water content and Loss-on-ignition

Water content is essential for determining sediment density and loss-on-ignition (LOI) at 550 °C can be used to estimate the organic content in the sediment. It can be further used to describe the quality of sediment (Salonen et al. 2002) and to assess the relation of allochthonous and autochthonous input to the environment (e.g. Nesje and Dahl 2001, Willemse and Törnqvist 1999).

Core ESGC1-13 was sampled with 1 cm interval for water content and loss-on-ignition. Each sample consisted of 1 cm^3 (app. 1.5 g) of wet sediment. The sediments were measured to pre-weighed crucibles and dried overnight in 105°C degrees. The weight loss equals to water loss and thus to the water content of the sediment. The original water content might not be resembled, as most reliable results of water content are analysed from cores immediately after collection. Unfortunately the core had quite a long storage time before sampling for this analysis, and some evaporation is likely to have happened, resulting in underestimation of water content and sediment porosity.

Dried samples were heated in 550°C degrees in a furnace for 2 hours to determine the LOI, as the organic content is burned away in the heating process (Dean 1974). Several factors can cause error to the measurement of LOI, such as sample size, exposure time and position of samples in the furnace (Heiri et al. 2001). For this reason sample size, exposure time and laboratory protocol was kept constant. Also other sedimentary components than the organic carbon can cause loss on ignition at 550°C, such as structural water of clay minerals, given that LOI is only a mere approximation of the organic content of the sediment.

4.1.2. Magnetic susceptibility

Magnetic susceptibility, reflecting the sediments capability to magnetize when subjected to an external magnetic field, may indicate several environmental perturbations (Thompson et al. 1975, Oldfield et al. 1983). The short cores were measured 1.–6.2.2014 at UNIS using Bartington *MS2* susceptibility meter with a surface scanning sensor *MS2*E1 (Bartington instruments Ltd, England). A standard protocol according to the manufacturers directions (Dearing 1999) was followed. Before measurements the cores were allowed to warm up to room temperature, a fresh surface was cleaned and covered with a thin plastic film to prevent contamination of the sensor. Drift checks were carried out prior to and after measuring the samples to verify the stability of the instrument and apply correction. Measurement of ESGC1-13 was conducted with a 0.5 cm interval while the other cores were measured with 1 cm resolution, all with high sensitivity range (0.1). For the top parts of the cores that were sub-sampled in the field, the susceptibility measurements were conducted directly on the bags. The samples were let to warm up and sediment was manually homogenized in the bags prior to measurement.

Possible error sources derive both from the core material and the measurement. The measurements were not possible to perform on a freshly split core, therefore the magnetic properties of the sediment may have altered during storage due to oxidation (Sandgren and Snowball 2001). The measurements can be affected by many external variables as the device is very sensitive, hence all known perturbations were minimized in the laboratory to stabilize the environment.

4.1.3. Spectrocolorimetry

Spectrocolorimetry allows quantitative colour measurements, non-destructively and with high resolution. The method, it's history and implications is outlined by Debret et al. (2011). Data processing can reveal valuable information on characteristics and components of the sediment not visible to bare eye, help facies analysis and function as a tool for interpreting sedimentary dynamics. Spectrocolorimetry is also an efficient tool for correlating related sediment cores.

Spectrocolorimetry measurements were carried out 6.8.–7.8.2013 at UNIS according to procedures in Debret et al. (2011). Measurements were conducted on a freshly cut and cleaned sediment surface. Due to the anoxic sediment character the cores were allowed to oxidize for at least an hour before the measurement to let the colour stabilize. The measurements were done directly on the core surface protected by a thin plastic film with portable Konica Minolta sensing CM-700d spectrocolorimeter. It is of major importance that the film does not alter the measured spectrum (Balsam et al. 1997, Chapman and Shackleton 1998), thus the reflectance was tested with international standard (ISO 7724-2) $BaSO_4$ calibration blanks. No alteration of the reflectance was detected. The ends of the cores were measured with extra care to prevent mixed signals with the tube filler material (green oasis) or to loose part of the signal with escaping light. The light emitted by the instrument was set to D65, corresponding to the temperature of 6504 K, which resembles daylight. For cores ESGC1-13, ESGC2-13 and ESGC3-13 the measurements were performed with 0.5 cm resolution, measuring interval of 0.2 cm and aperture of 0.5 cm. Rest of the cores were measured with 1 cm resolution, 0.5 cm interval and 0.8 cm aperture. To accept the data the calculated amount of data points had to match the actual amount of measurements. All high resolution and selected lower resolution measurement were repeated to assure the quality of the data.

Natural colour change in anoxic sediment may serve as a source of error if the colour had not completely stabilized prior to all measurements. However, the time given is considered sufficient (Maxime Debret, personal communication, 2013). During the laboratory experiments changes in water content may appear due to evaporation. Moisture affects the sediment colour, and in fine-grained sediments changing water content also alternates the composition of the sediment (Balsam et al. 1998).

4.2. Chronologic methods

For the chronology of the core two methods of dating were explored. For the top part stable isotope chronology of ^{210}Pb and ^{137}Cs was conducted in the sediments and throughout the core radiocarbon analysis was performed on terrestrial plant macrofossils.

4.2.1. Radiocarbon dating

From the core ESGC1-13 ten plant macrofossil samples were chosen for the accelerator mass spectrometer (AMS) radiocarbon analysis. Samples were picked from depths of 5–5.5, 10–10.5, 13.8, 18.6, 31.3, 40.2, 42.7, 43.6, 46.6 and 56.1 cm (see also Table 3.), representing a relatively even distribution and good coverage over the whole core length. All samples are terrestrial species, primarily bryophytes, sufficiently sized, and thus considered to be well suited for the analysis. The samples were analysed in the Tandem Laboratory of Uppsala University, Sweden. A standard protocol of acid-base-treatment was carried out at the dating laboratory prior to AMS-measurement.

Quality of dated material is crucial to the resulting chronology. Terrestrial macrofossils represent a single carbon reservoir tightly connected to the atmospheric carbon cycle and result in higher accuracy compared to bulk sediment samples, which are prone to errors caused by mixed carbon sources (Oldfield et al. 1997, Barnekow et al. 1998), or dating of aquatic macrofossils which may suffer from contamination of old carbon dissolved from the surrounding bedrock on carbonate areas (hard-water effect) yielding considerably older, erroneous ages (Wolfe et al. 2004).

4.2.2. Fallout radio nuclides: ^{210}Pb and ^{137}Cs

To evaluate the temporal context of the youngest sediments analysis of ^{210}Pb and ^{137}Cs was performed, method is useful for dating recent sediments in environmental studies (Appleby 2001, 2008). It is based on the concentration of the natural radioisotope ^{210}Pb (halflife 22.3 yrs.) accumulating to lake sediments from the atmosphere on a constant rate, but due to local variation on natural occurence and rainfall technique requires careful site-specific calibration. This is regularly done with the aid of ^{137}Cs, which deposits from the atmosphere in a similar manner to ^{210}Pb but is an artificial nuclide produced by nuclear reactions. Two peaks are evident in a well preserved ^{137}Cs record from Northern Hemisphere: a peak of atmospheric nuclear weapon testing in 1963 and the Chernobyl reactor accident in 1986 (Appleby 2001). Main possible error sources are deficient sediment density data and sediment mixing, due to for example bioturbation or chemical diffusion (Appleby 2001, 2004).

Dated material included sediment aliquots of core ESGC1-13 on 0.5 cm resolution: of the surface sediment extruded at the field site for 0–10 cm and for 10–20 cm collected from the split core. Samples were analyzed in The Liverpool University Environmental Radioactivity Research Centre (ERRC) and modelled with a constant rate of supply (CRS) model (Appleby and Oldfield 1978) in two sections (Appleby 2001).

4.4.3. Age-depth model

The age-depth model was built with Clam 2.2, a classical age-depth modelling program run in statistical software R (Blaauw 2010). Calibration of radiocarbon was based on IntCal13 curve and for the samples including modern carbon on a northern hemisphere postbomb curve suitable for arctic specimens (region 1). Age-depth model was run with 1000 iterations of a smooth spline function (smooth 0.3) and extrapolated in the lower end to cover the full core length.

4.3. Chironomid analysis

Subfossil remains of chironomids were analyzed in order to trace the community development and related changes in environmental conditions. The standard procedures of chironomid analysis (e.g. Walker 2001, Brooks et al. 2007) were applied. The 64 cm long deep basin surface core ESGC1-13 was analysed with continuous 1 cm resolution. From each interval 2–4.5 cm^3 of wet sediment was sieved through a 100 μm mesh in running water and distributed to a Bogorov sorting tray (Gannon 1971). All head capsules in each sample were picked under stereomicroscope at x40 magnification. Capsules were transferred directly to microscopy slides ventral side up and mounted in Euparal®. Taxa was identified under a light microscope (x200–400) with a minimum of 50 head capsules per sample to provide sufficient statistical significance (Heiri and Lotter 2001, Quinlan and Smol 2001b).

Identification of fauna is based on Brooks et al. (2007). As a primary choice identification is based on the composition of the mental teeth crown, which differs between morphotypes in the number, relative size and assemblage of teeth (Brooks et al.

2007). Other characteristic parts of the head capsule, including ventromental plates, mandibles, antennal pedestals, post-occipital plate and setae, and general habitus are used in equal manner when applicable.

Identification itself is naturally a possible source of error. Samples were picked and analyzed in a random order to minimize any within-record bias caused by the developing skills of the taxonomist. Due to high local variation of the chironomidae the appearance of a certain species' head capsule might vary considerably in comparison with ones found in other locations (Dr. Tomi Luoto, personal communication, 2013). This makes visually based identification more challenging, as primary attributes including teeth, can show slightly different morphologies. In addition variability between instars can be misleading. Identification of broken and wrinkled capsules is often complicated and is based on what is left of the distinct features.

4.4. Data analyses

4.4.1. Principal component analysis

Principal component analysis (PCA) of relative chironomid abundance data was used to detect patterns and relationships between the chironomid community and environmental variables. PCA, a linear indirect ordination method, was used for describing the relationship between chironomid assemblage and environmental variability. PCA component 1 scores were also used to assess units in the chironomid community. The analysis was done with Paleontological Statistics (PAST) beta program for OSX (Hammer et al. 2001).

4.4.2. Diversity indices

Taxonomic diversity was evaluated by using several statistical measures that describe different aspects of the chironomid assemblage. Here the family of Hill's numbers (Hill 1973) is used as a guideline. Hill's N2 index was used to describe species evenness (Hill 1973, Tuomisto 2010) and Shannon's H index to indicate entropy within the assemblage

(Jost 2006). Hill's N2 reflects the variation within very abundant taxa and Shannon index, which is directly related to Hill's N1 (N1=e^Shannon), depicts the variation within abundant taxa (Hill 1973). Species richness is simply demonstrated as the number of taxa in each sample, which is also know as the Hill's N0. PAST (Hammer et al. 2001) was used to calculate the species richness and Shannon values. For Hill's N2 index the program C2 (Juggins 2003) was used.

4.4.3. Cluster analysis

To statistically assess community development and ecological turnovers, a cluster analysis was performed on relative abundance data of chironomids. Analysis was calculated with a paired group (UPGMA) algorithm based on chord distance as similarity index and the cophenetic correlation coefficient of 0.4. For the calculations PAST (Hammer et al. 2001) was used.

4.4.4. Correlation coefficients

Relationships between physical parametres (LOI, chlorophyll *a* derived productivity, magnetic susceptibility), chironomid inferred temperature reconstructions and biological data (PCA axis 1 and 2 scores, relative abundance of main species and diversity indexes) were assessed by calculating correlation between them. Spearman's (r_s) correlation coefficients, with associated levels of statistical significance (p), were calculated with the PAST program (Hammer et al. 2001).

4.4.5. Chironomid inferred temperature reconstructions

The analysed relative abundance chironomid fauna was used to reconstruct past variations in air temperature. Summer air temperature is one of the most significant factors affecting the distribution of chironomid taxa and the highest correlation has generally been found with mean July air temperature within Northern hemisphere (Eggermont and Heiri 2012). Two alternative reconstruction approaches were tested.

One reconstruction is based on a Norwegian training set (Brooks and Birks 2001), which consists of 157 Norwegian lakes from different latitudes and altitudes, including lakes from Svalbard, with an air temperature range of 3.5–16.0 °C (Heiri et al. 2011). A version of the Norwegian training set compatible with the taxonomy presented in Brooks et al. (2007) was applied. 22 identified taxa was used in the reconstruction, excluded speciestypes were *Microspectra contracta*, *M. junci, Cricotopus obnixus* and *Chironomini spp*. (unidentified) were not present in the training set. Unidentified categories *Hydrobaenus sp*., *Hydrobaenus*/*Orthocladius* and *Cricotopus*/*Orthocladius* were merged in one. For the reconstruction a weighted-average partial least squares (WA-PLS) model was used.

The second reconstruction is based on a North-eastern Canadian training set (Francis et al. 2006), which comprises 68 sites and 44 taxa from northern Canada. The calibration set represents a mean July air temperature range of 5.0–19.0 °C. The taxonomic resolution of the training set is lower than in the analyzed assemblage, consequently some taxa were clustered to be compatible with the training set as seen in Table 2. A WA-model (weighted averaging) with tolerance down weighting and classical deshrinking was the best perfoming approach.

Table 2. Taxonomical grouping performed to the Ellasjøen chironomid assemblage in order to make it compatible with the North-eastern Canadian training set (Francis et al. 2006).

Francis training set category	**Ellasjøen assemblage**
Subtribe Tanytarsina	*Microspectra radialis, M. insignilopus, M. contracta, M. junci, Paratanytarsus austriacus*
Heterotrissocladius	*Heterotrissocladius maeaeri, H. grimshawi*
Cricotopus/Orthocladius	*Ortocladius consobrinus, O. trigonolabis, O. type S, Cricotopus intersectus, C. obnixus, C. type P, Cricotopus/ Orthocladius*
Eukiefferiella/Tvetenia	*Eukieffiriella*
Corynoneura/Thienemanniella	*Corynoneura arctica*
Oliveridia/Hydrobaenus	*Hydrobaenus lugubris, Hydrobaenus sp., Hydrobaenus/ Orthocladius*

The reliability of temperature reconstructions was assessed by calculating the percentage of fossil taxa represented in the training set (cut-off value 95% for good representativeness) and for the Norwegian training set by examining the distance of modern analogues between fossil and training set samples using the modern analogue technique (MAT). A good analogue was considered to have a chord distance less than the upper 90% confidence interval of the mean minimum dissimilarity coefficient of the training set.

5. RESULTS

5.1. Physical properties

5.1.1. Water content and LOI

Results of the water content show fluctuating trends ranging over values 59–76 % (Fig. 9.). In the lower part of the core water content values show rather trendless fluctuation of 60–70 % with generally higher values between 46–28 cm (1330–1550 AD). The most pronounced change occurs at 27–26 cm (~1550 AD), featuring the lowest value of 59 % and the starting point of a rapidly increasing trend towards the surface. Water content is the highest towards the top of the core, 76 % at 11-10 cm (1700 AD), and above 10 cm 89 % on average.

The Loss-on-ignition shows trends very similar to water content with values fluctuating between 8–13 % as seen in Figure 9. The lowermost part of the core (64–53 cm, 850–1150 AD) features slightly higher than average values. Lower values between 53 and 46 cm (1150–1330 AD) are followed by a straight trend with alternating but generally higher values between 46 and 28 cm (1330–1550 AD). A distinct peak occurs at 43.5 cm (1360 AD), which correlates with a sediment horizon rich in moss remains. The most prominent change happens at 27–26 cm (~1550 AD), where the minimum value of

8 % is reached, followed by a clear increasing trend towards the top. The highest values are found towards the surface.

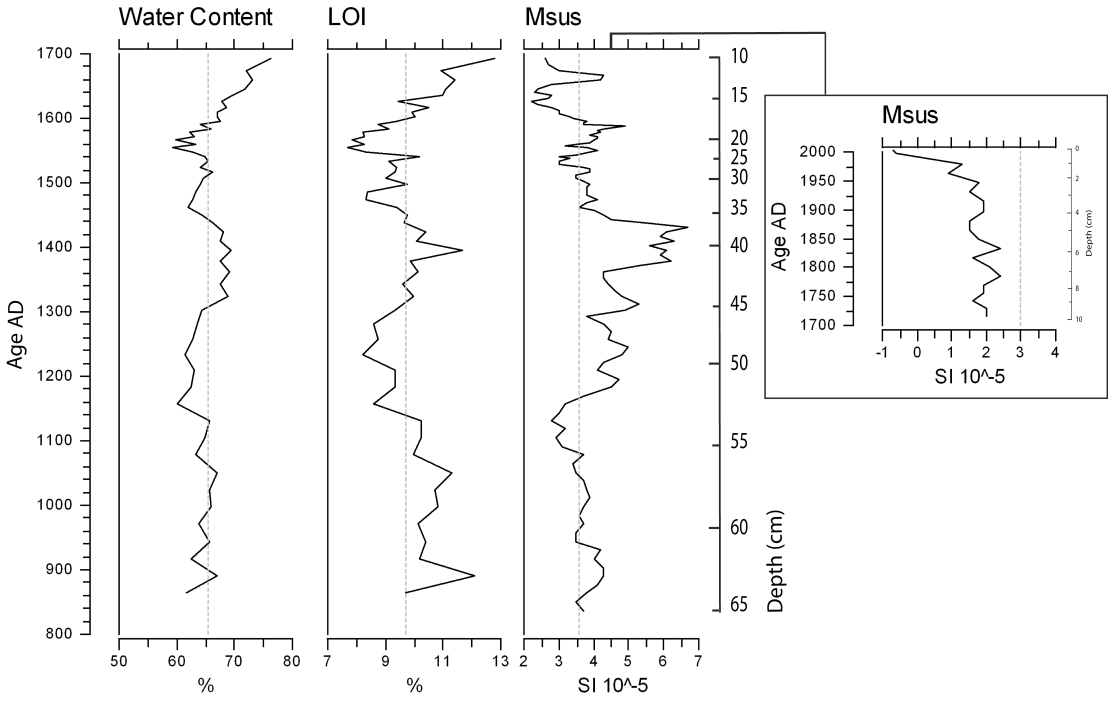

Figure 9. Results of water content, loss-on-ignition (LOI) and magnetic susceptibility (Msus) through the core, for Msus also sub-sampled top 10 cm is shown. Average value of the series is marked for each variable (grey line).

5.1.2. Magnetic susceptibility

The magnetic susceptibility results alternate in the range of 2.2–6.7 SI 10^{-5} (Fig. 9.). The bottom part of the core (64–51 cm, 850–1200 AD) features average values. A clear trend increasing towards the top is observed between 51 cm and 38.5 cm (1200–1440 AD), peaking as a prominent interval of high values (> 5.6 SI 10^{-5}) at the depth of 42–38.5 cm (1390–1440 AD). The shifts in magnetic susceptibility at 38.5 cm and 51 cm are rather abrupt. The trend in magnetic susceptibility is decreasing above 38.5 cm (1440 AD) with a couple higher intervals and the lowest values are reached at the surface.

5.1.3. Spectrocolorimetry

The spectrocolorimetry data was processed in three ways to investigate the sedimentary components and processes: as a down core profile of first derivative values (FDS) of the visual spectra, as a Q7/4 diagram and as calculated chlorophyll *a* signature.

The FDS-spectrum through the length of the core, except for the field-extruded part where measurements were not carried out, is shown in Figure 10. Compounds peak at their characteristic wavelengths in the FDS-spectrum, thus allowing a quick look on the dominant components of the sediment's spectra. The most pronounced reflective signal in ESGC1-13 is reached at 555 and 565 nm which are peaks indicating iron oxide compounds, namely hematite. The hematite signal shows marked variability down core, with bulk of the values between 0.06 and 0.07. Lowest values are experienced in the very bottom of the core (0.04), whereas two highest peaks reach up to 0.082 and 0.076 at 49 cm (1240 AD) and 27 cm (1550 AD) depth respectively. Other iron compounds visible in the spectra are iron oxyhydroxides such as goethite peaking at 435 nm and 525 nm. Goethite reflectance is distinctly lower in the core below 52 cm (1170 AD) and higher at 27–10 cm (1550–1700 AD) depth, accompanying all the higher hematite peaks.

The second highest reflectance peak is experienced close to 700 nm, representing the organic components in the sediment (Fig. 10.). Values are mainly ranging between 0.04 and 0.05. However, there are distinct drops in the reflectance values at 42–40 cm (1390–1420 AD) and especially 20–15 cm (1600–1630 AD), where the values are below 0.04. While almost all the measurements peak close to 700 nm, the gradient of the organic reflectance is varying. For the lower part of the core this signal is alternating. At 10–20 cm (1600–1700 AD) interval organic wavelengths of 675 nm and shorter show lower reflectance. The FDS-spectrum does not show any distinct carbonate signature, as carbonates would dominate the reflectance on the short wavelengths (400–550 nm).

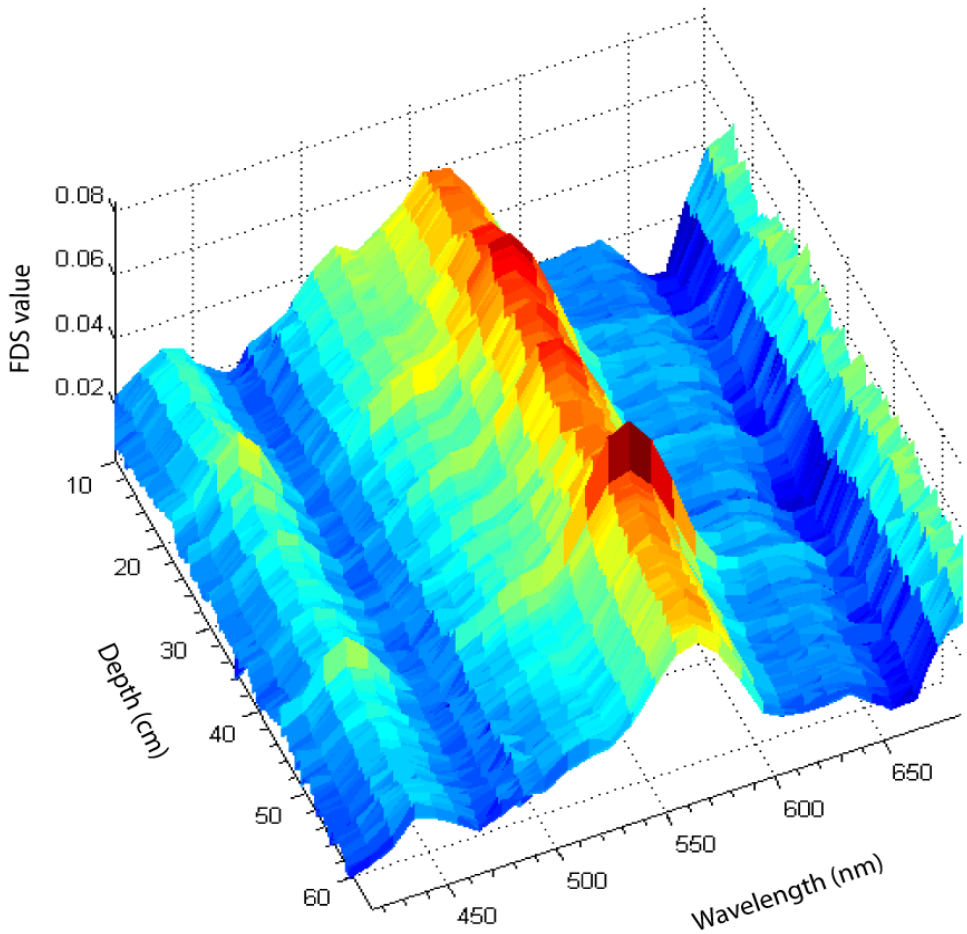

Figure 10. First derivative values of the visual spectra of core ESGC1 displayed in 3D against depth and wavelength. Hematite reflectance is the highest, observed at 550 nm. Another distinct peak are the organic compunds close to 700 nm.

For a better look into the sedimentary components a Q7/4 diagram was produced from the spectrocolorimetric data (Fig. 11.). The samples feature fairly homogenous lightness (L*) values between 30–40 % and Q7/4-ratios ranging from low to relatively high (~2 to ~4.5).

Most data points group together densely in the diagram spreading mainly between poles A ("clayey deposits") and B ("chlorophyll *a* and by products or organic rich products") as described by Debret et al. (2011) (Fig. 11.). When physical proxy units (see chapter 5.2.) are applied to the Q7/4 data, a trend from more clayey (pole A) towards more primary production dominated sediment (pole B) can be clearly seen. A few measurements in units 1 and 2 draw also towards pole C ("altered organic matter"). Unit 3 features slightly higher than average L* values, remaining steadily on the side of the

less organic and more minerogenic sediment signature. FDS-spectrums typical to each unit were inspected for possibility of spectral muting, which would hinder the functionality of Q7/4 diagram when two high reflectance peaks would average each other out in the diagram. No muting was detected, and the spectrums with their fine between-unit differences are displayed in Figure 11.

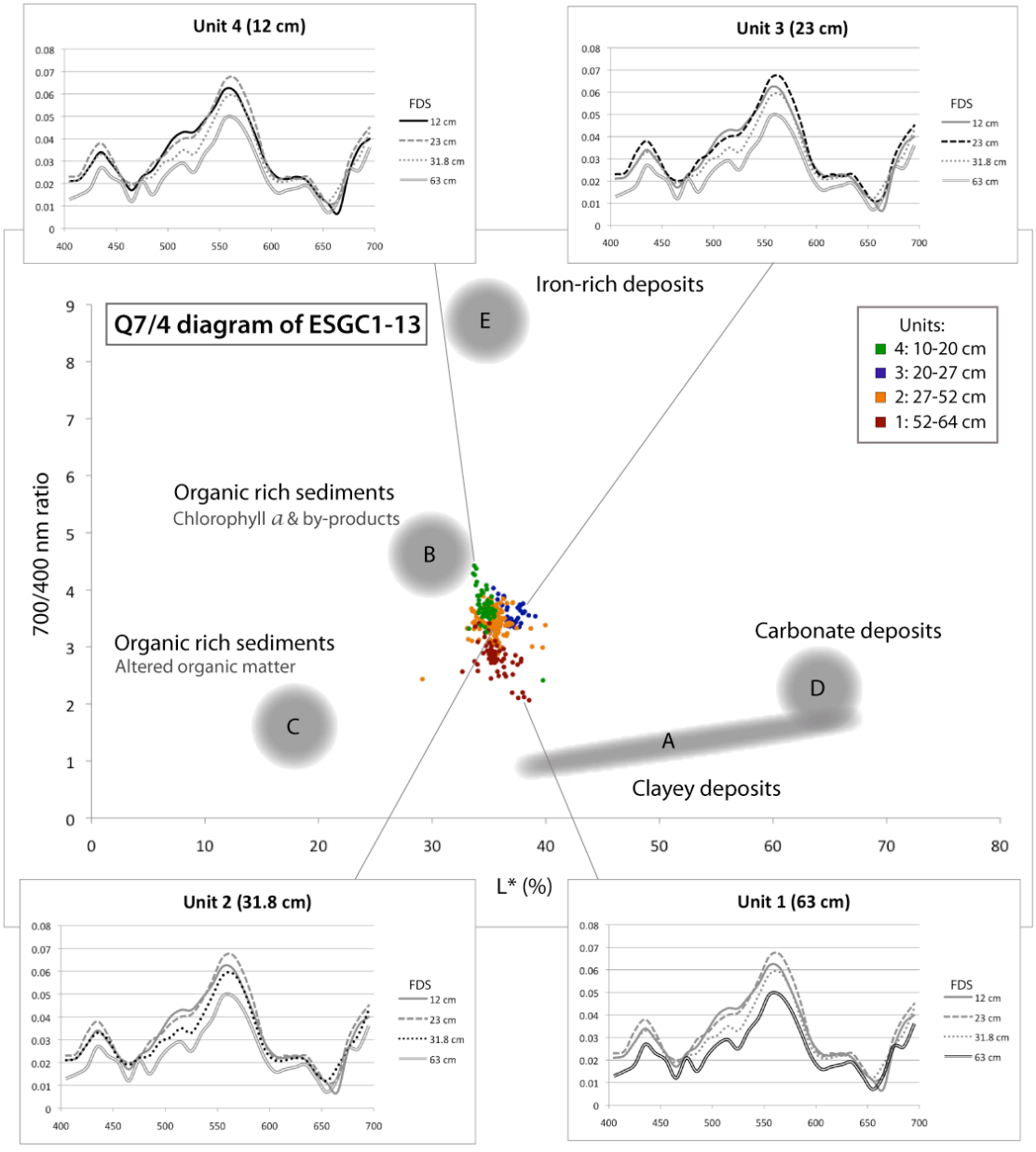

Figure 11. The data points from ESGC1 are clustered in the middle of Q7/4 diagram, drawing between clayey and organic rich deposits. Physical proxy units highlight the changes in depth: a clear succession from more clayey to more chlorophyll *a* rich sediment is evident. Poles (A-E) are presented as described by Debret et al. (2011). The surrounding four FDS spectrums demonstrate a typical reflectance for each unit (in black) against the other units (in grey).

Spectrocolorimetry also allows semi-quantitative determination of chlorophyll *a*, which has reflectance of 675 nm, and was calculated according to Wolfe et al. (2006) to include also derivative compounds. Chlorophyll *a* reflectance features an alternating trend and is clearly lower around 40 cm (~1420 AD) and at 10–20 cm (1600–1700 AD) interval (Fig. 12.).

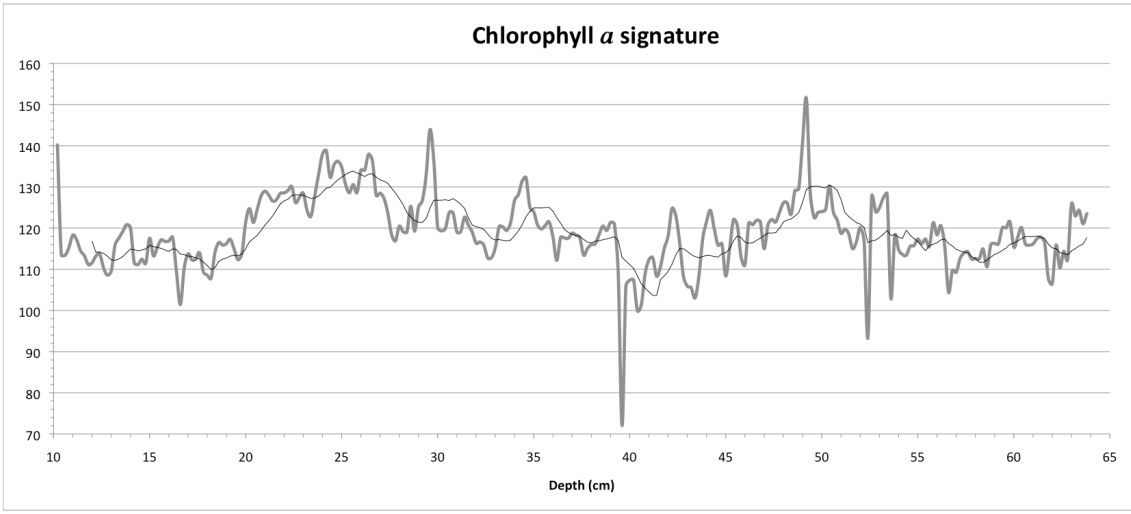

Figure 12. The spectral signal of chlorophyll *a*, which gives an estimation of primary production development within the lake (Wolfe et al. 2006). Actual values (grey line) and a 10 period moving average are displayed.

5.2. Sedimentary units

Based on the patterns of the FDS-spectrum, the other physical proxies (magnetic susceptibility, LOI and water content) and the core lithology, four units were identified (Fig. 13.). Unit 1 (64–54 cm, 850–1120 AD) clearly shows the least variation at any parameter. Magnetic susceptibility is slightly decreasing while chlorophyll *a* reflectance is rising.

Unit 2 (54–27 cm, 1120–1550 AD) is the longest and most heterogeneous. The lower boundary at 54 cm is represented as a drop of values in all physical proxies and correlates with a white horizon in the core. It is characterized by generally higher

hematite and organic reflectance. Magnetic susceptibility is strongly increasing until 38.5 cm (1440 AD) where an abrupt drop initiates a decreasing pattern, again the chlorophyll *a* signature follows with opposite trends. Water content and LOI feature fluctuating, trendless values.

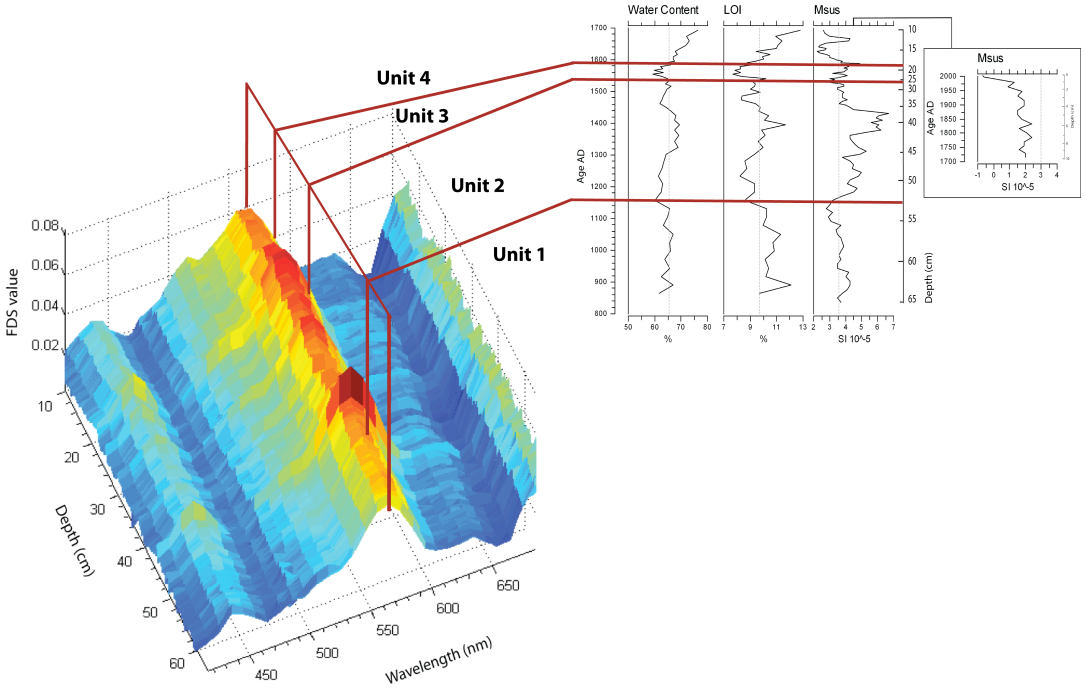

Figure 13. The core ESGC1 was divided into four units according to the FDS spectrum and physical properties as shown.

Unit 3 (27–20 cm, 1550–1600 AD)) displays the highest sustained iron reflectance in the material, depicted also in rising magnetic susceptibility. Also the organics and chlorophyll *a* feature constantly high reflectance. The lower unit boundary correlates with a dense, white marker horizon in the lithology, which also explains the dip in LOI and water content values, as well as the respective peak in magnetic susceptibility. Unit 3 defines an interval of particularly high sedimentation rate.

Unit 4 (10–20 cm, 1600–1700 AD) is characterized by overall homogenous values in the FDS-spectrum. Organic compounds show reflectance values below core average but feature an increasing trend, yet chlorophyll *a* signature remains low. Magnetic susceptibility follows a decreasing trend while water content and LOI are rising.

5.3. Chronology

Radiocarbon method was applied on ten terrestrial macrofossils, results are shown in the Table 3. Most ages derived follow the sedimentation in a logical order, and age reversals occur only in the lower part of core between samples Ua-47865 and Ua-47866. Specimens Ua-47864 and Ua-47865, displaying considerably older ages than other samples are considered as outliers.

Table 3. Radiocarbon dates from 10 macrofossils chosen from ESGC1. Samples Ua-47864 and Ua-47865 are considered outliers.

Lab number	Depth (cm)	Type	Species	^{14}C age BP	∂^{13}C‰ VPDB
Ua-47857	5-5.5	moss	*Sanionia orthothecioides*	*114.1±0.6 pMC*	-25*
Ua-47858	10-10.5	twig	-	*137.7±0.6 pMC*	-29.2
Ua-47859	13.8	moss	*Aulacomnium turgidum*	264±30	-25.8
Ua-47860	18.6	moss	*Racomitrium lanuginosum*	270±31	-25.4
Ua-47861	31.3	moss	*Scorpidium cossoni*	342±37	-25*
Ua-47862	40.2	moss	*Polytrichum alpinum*	525±30	-24.5
Ua-47863	42.7	moss	*Racomitrium lanuginosum*	542±32	-24.5
Ua-47864	43.6	moss	*Philonotis caespitosa + Calliergon sp.*	1800±40	-24.2
Ua-47865	46.6	moss	*Racomitrium lanuginosum*	4138±42	-26.2
Ua-47866	56.1	moss	*Racomitrium lanuginosum*	995±30	-23.4

* Assumed value

The ^{210}Pb dating was carried out in the uppermost 20 cm. Results are shown in Appendix 1. The results suggest, that supported levels of ^{210}Pb were reached at about 20 cm depth, and the finished model dates back to 1883 AD at 17.25 cm.

Chronology of the core was assessed with an age-depth model based on eight radiocarbon samples (Fig 14). The outlying dates Ua-47864 and Ua-47865 (see Table 3.) were excluded from the model, and the ^{210}Pb results are presented as outliers due to major discrepancy. For further evaluation of the model see discussion in chapter 6.1.1.

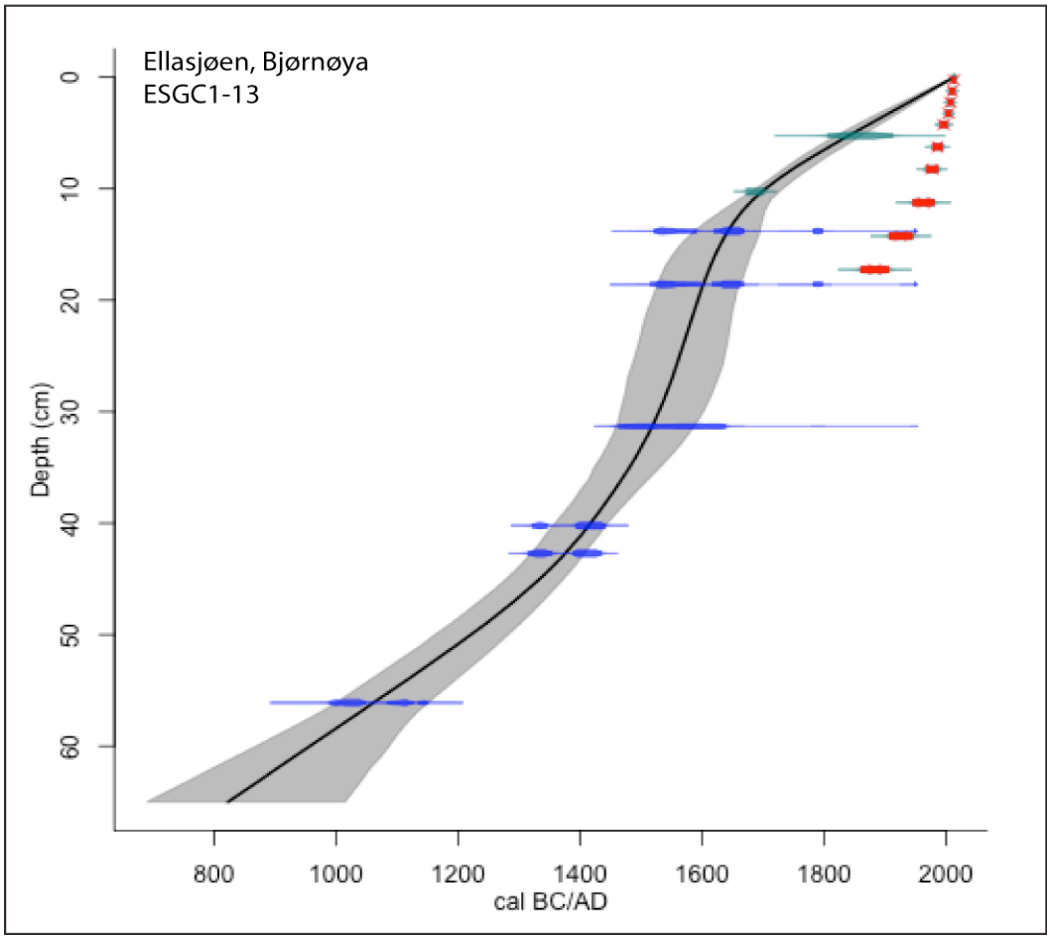

Figure 14. A smooth spline age-depth model of ESGC1 based on radiocarbon results. Traditional (blue) and modern carbon (turquoise) calibrated ages with error margins are displayed. Grey shaded area refers to 2σ confidence range. Alternative 210Pb chronology is presented (red) and outlying samples Ua-47864 and Ua-47865 are excluded.

5.4. Chironomid assemblages

In total 29 chironomid taxa were identified from Ellasjøen. Throughout the studied interval the most dominant species groups are *Heterotrissocladius maeaeri*-type composing 30-80 % of the population and *Microspectra radialis*-type (7–39 %). In smaller numbers *Paratanytarsus austriacus*-type (average relative abundance 6 %), *Orthocladius consobrinus*-type (3 %), *O. trigonolabis*-type (2 %), *O. type S*-type (2 %), *H. grimshawi*-type (1 %) and *M. insignilobus*-type (1 %) occur throughout the core. Complete taxonomy is presented in Figure 15. as relative abundances and pictures of key taxa can be seen in Appendix 2.

The chironomid community is relatively constant through the investigated time period, and ecological shifts are reflected in changes of the relative abundances rather than introduction or disappearence of taxa. The lowermost part of the core (64–52 cm, 850–1170 AD) is characterized by high abundance of *H. maeaeri*-type (~59–79%) and *M. radialis*-type (~14–22 %), very low abundance of *P. austriacus*-type (~1–2 %), absence of *M. contracta*-type and the highest within-core occurrence of *Diamesa zernyi/ cinerella*-type of up to 3.5 %.

At 52–39 cm (1170–1440 AD) *H. maeaeri*-type shows a declining trend towards the top, however with relative abundances still higher than 50 %. Occurrence of *M. radialis*-type fluctuates at ~14–36 %. Characteristic to this interval is the gradual increase of *P. austriacus*-type from <1 % to approximately 10 %, and introduction of *M. contracta*-type (~0–5 %). *H. grimshawi*-type is absent in the lower part of the zone but re-occurs again at 44 cm.

The interval of 39–13 cm (1440–1650 AD) is characterized by constant trend but high fluctuation in all present taxa. Above 20 cm (1600 AD) *H. maeaeri*-type starts to decrease and *M. radialis*-type increase. As average abundances in the zone *H. maeaeri*-type is the most abundant with 66 %, followed by *M. radialis*-type (18 %) and *P. austriacus*-type (6 %). Between 37–18 cm (1460–1610 AD) occurrence of *O. consobrinus*-type is low (~1 %), a third of the full profile's average.

A shift occurs at 13 cm (1650 AD), when the abundance of *H. maeaeri*-type drops from 64 % to 43 % and *M. radialis*-type increases from 18 % to 33 % instantaneously. The uppermost part of the core (13–0 cm, 1650–2013 AD) shows much more even distribution between *H. maeaeri*-type (~40 % on average) and *M. radialis*-type (~29 %) than any other interval. *M. radialis*-type peaks at 10–8 cm (1700–1760 AD) for a momentary dominance of the taxa. Occurrence of *P. austriacus*-type and *M. contracta*-type increases markedly at 10 cm depth (1700 AD). Towards the surface *Cricotopus intersectus*-type begins to occur regularly while *H. grimshawi*-type diminishes and *O. trigonolabis* -type disappears from the assemblage.

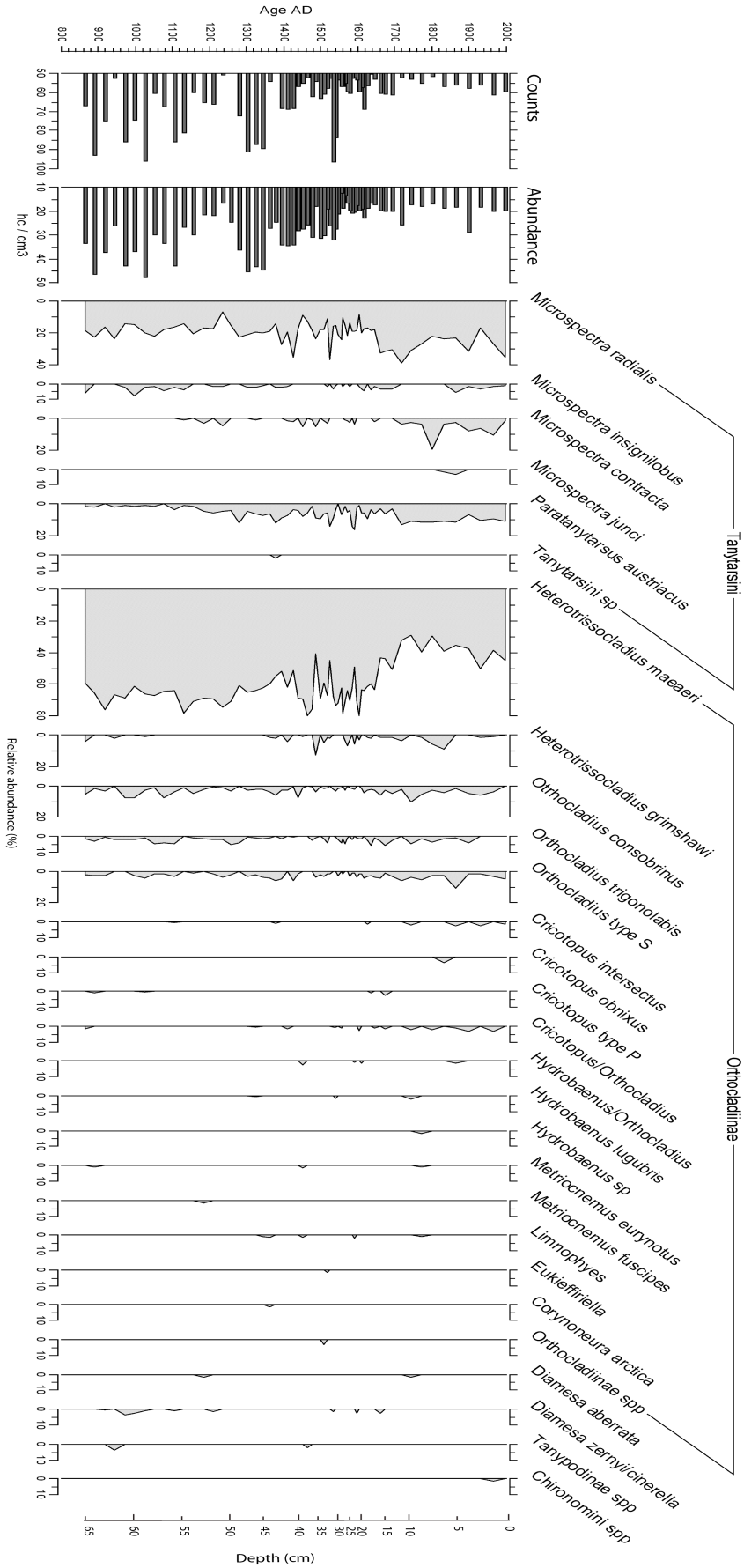

Figure 15. The chironomid fauna in Lake Ellasjøen as relative abundances.

The homogenity of the assemblage allows various unit divisions (Fig. 16.). Cluster analysis offers different options with different similarity indexes, but most clearly suggests unit divisions 0–13 cm (1650–2013 AD), 13–30 cm (1530–1650 AD) and 30–64 cm (850–1530 AD) with 0.43 Chord distance. Sample scores of PCA component 1 can also be used to describe units as 0–13 (1650–2013 AD) cm features distinctly negative values, 13–43 cm (1370–1650 AD) highly variable values and 43–64 (850–1370 AD) cm positive values. The most distinct unit depicted by cluster analysis, PCA component 1 values and visual assessment is the top 0–13 cm (1650–2013 AD). In this study the PCA based units are applied further due to their clear climate association.

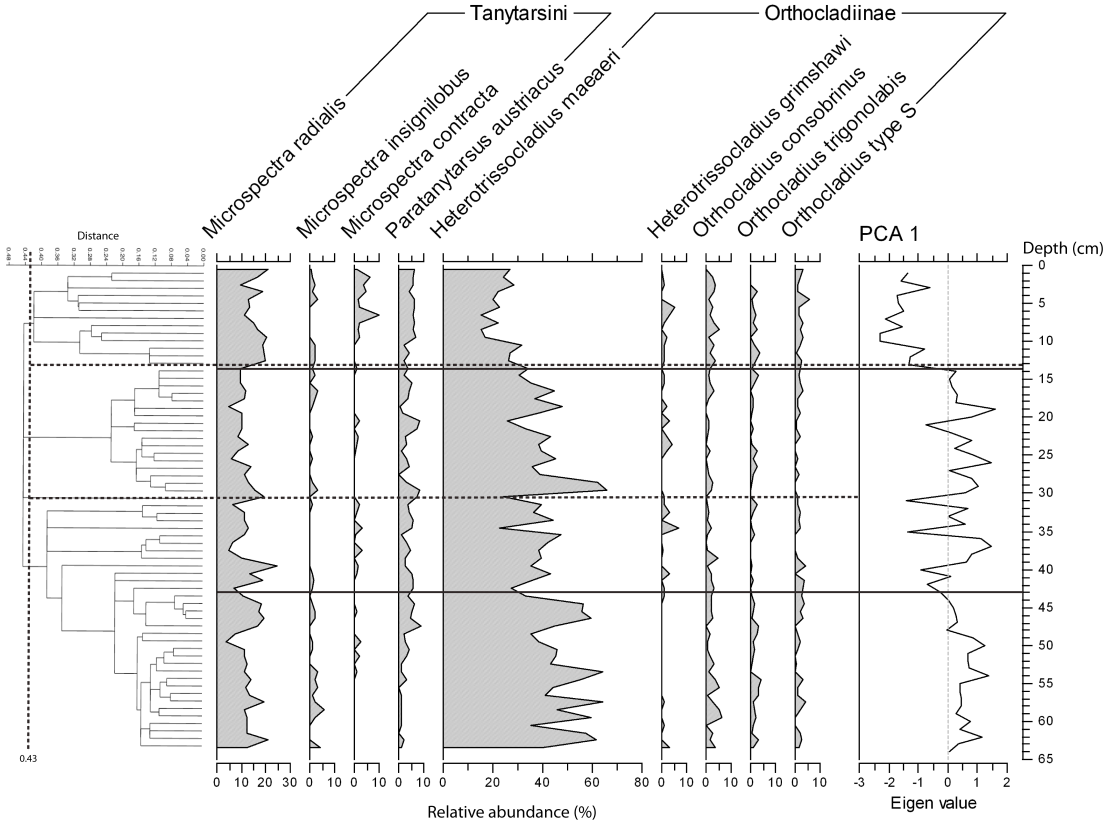

Figure 16. Optional unit divisions of biological assemblage based on cluster analysis or PCA component 1 association. Most common taxa in Ellasjøen is presented for referance.

The abundance of chironomids in the sediment is approximately 30 head capsules (hc) per cm^3 of wet sediment below 27 cm (1550 AD), peaking at 57–58 cm (~1000 AD) as >48 hc/cm^3. However, there is a very distinct drop in abundance at 49-50 cm (~1230 AD) depth (<20 hc/cm^3). At 26–27 cm (~1550 AD) the abundance suddenly drops to the minimum of <13 hc/cm^3. Above 26 cm (1560 AD) the abundance is about 20 hc/cm^3.

5.5. Data analyses

5.5.1. Principal component analysis

Samples are relatively scattered in the principal component analysis of chironomid assemblage (Fig. 17.). PCA component 1 explains 78.6 % of the variance in the assemblage. Component 2 explains 8.8 % of the variance, thus together axis 1 and 2 explain 87.4 %.

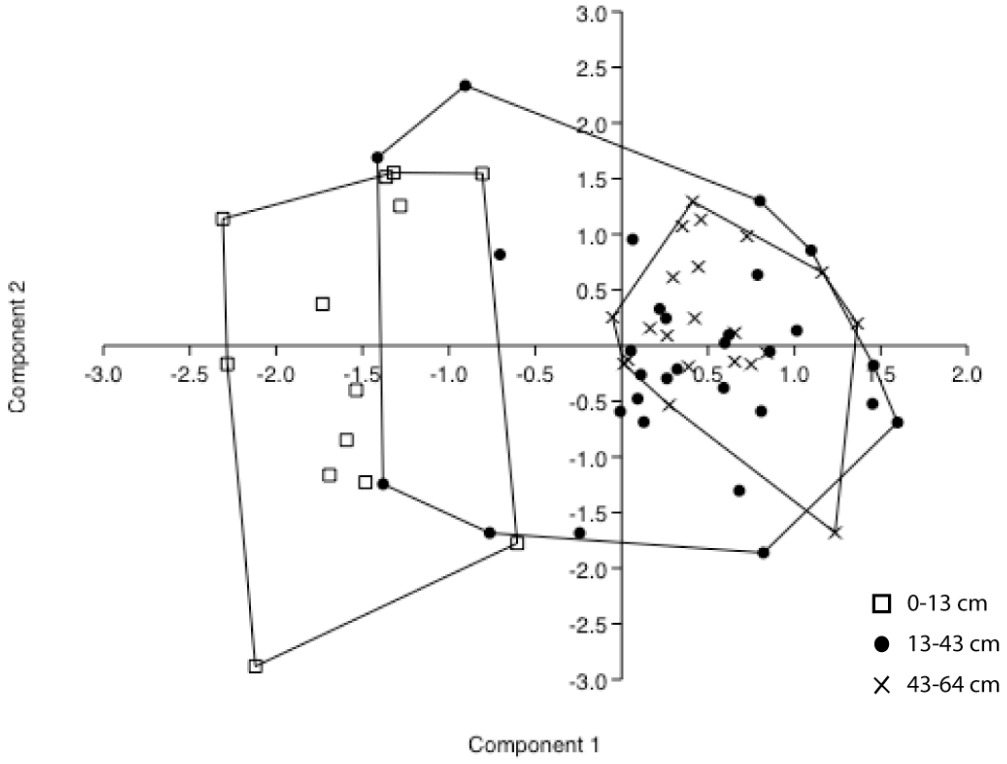

Figure 17. PCA sample scores of chironomid assemblages in ESGC1. Samples are clustered according to depth zones. Population development proceeds towards negative component 1 values.

When the biological intervals described before are applied to the PCA a clear negative trend along axis 1 can be seen. Oldest samples (43–64 cm, 850–1370 AD) cluster comparatively densely on the positive side of axis 1. The second unit, 13–43 cm (1370–1650 AD), spreads around the oldest unit drawing towards more negative values of axis

1. The youngest samples (0–13 cm, 1650–2013 AD) are located distinctly on the far negative axis 1 end of the PCA plot, overlapping only with a few samples from unit 2.

As seen from the PCA biplot (Fig. 18.), *Heterotrissocladius maeaeri*-type has a positive association with components 1 and 2 while *Microspectra radialis*-type has a strong positive association with component 2 but a negative one with component 1.

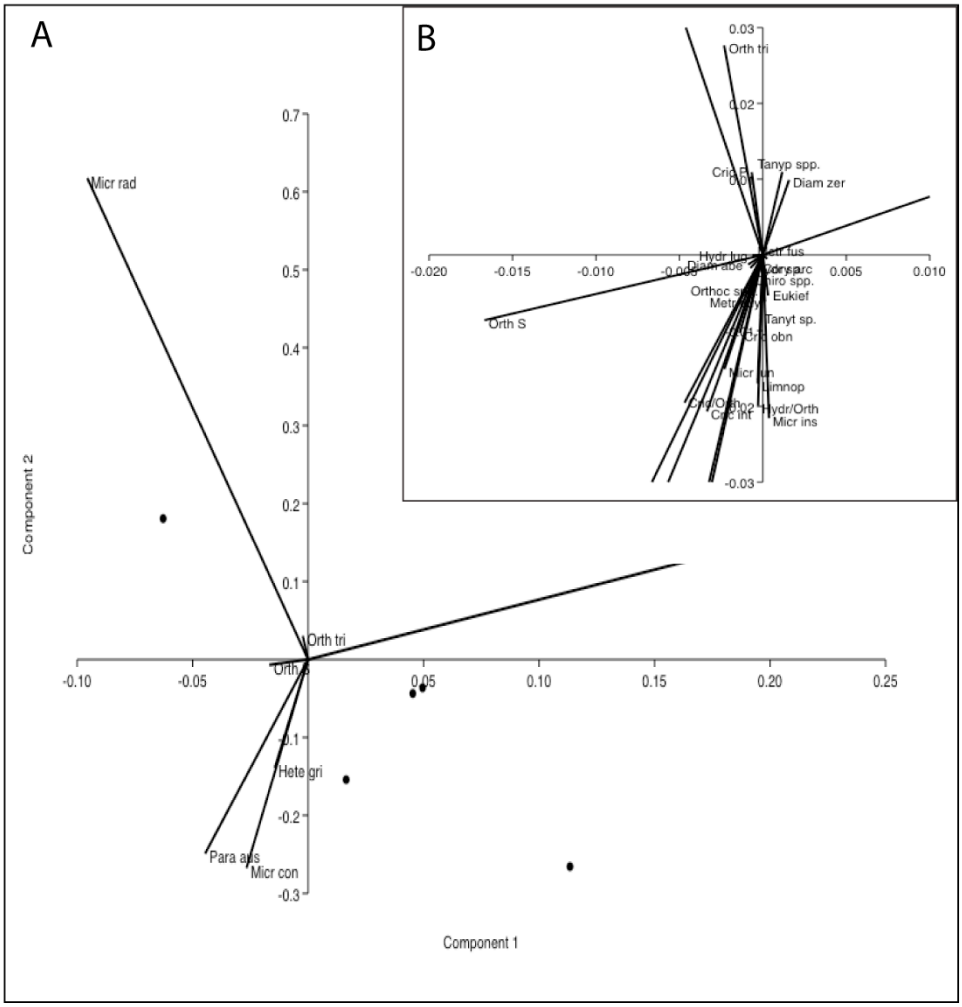

Figure 18. PCA biplot of chironomid samples (dots) and taxa (lines). Due to scaling only a few samples are displayed. A. Responses of main speciestypes *H. maeaeri*, *M. radialis*, *P. austriacus* show a different response to components 1 and 2. B. A close up, where weakly responding taxa is mainly seen to fall into negative correlation area with both components. Taxonomic abbreviations are based on four first letters of genus and three first letters of the speciestype name, with the exceptions of *Orthocladius type S* (Orth S), *Cricotopus type P* (Cric P), *Limnophyes* (Limnop) and *Eukieffiriella* (Eukief).

5.5.2. Diversity indices

Species richness in the chironomid assemblage is highly variable, ranging from 4 to 12 taxa in a sample (Fig 19.). Species richness is lower in the bottom part of the core and higher towards the top. From approximately 15 to 1 cm (1630–1980 AD) depth the diversity is consistently at highest on average.

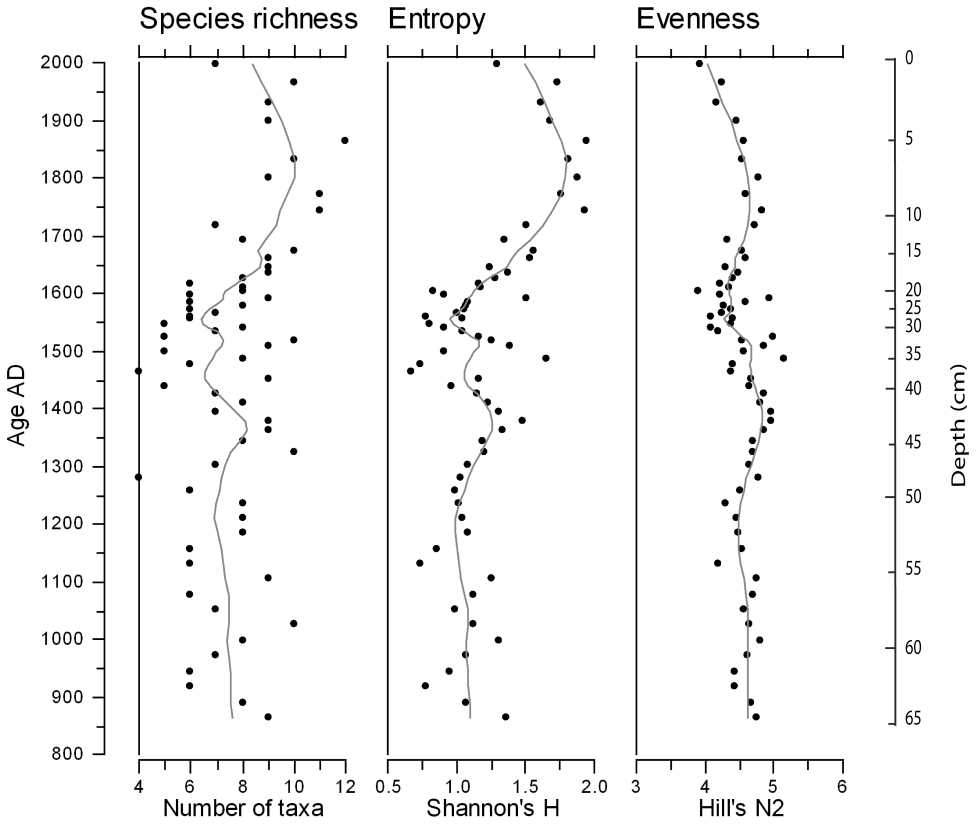

Figure 19. Species richness (number of taxa), entropy (Shannon's H) and evenness (Hill's N2) of the fossil chironomid assemblage in lake Ellasjøen are presented. The line indicates a locally weighted smooth (lowess, span 0.2) of the sample specific scores (dots).

Shannon index follows a similar pattern to species richness, ranging between 0.7 and 1.9. The values are fluctuating but clearly elevated above 18 cm depth. At ~6–18 cm (1610–1810 AD) entropy clearly increases in the assemblage followed by a decline towards the present.

Hill's N2 index shows more concentrated values compared to the other diversity indices. The pattern of fluctuation follows the Shannon index and roughly the species richness, but the elevated values between ~7–18 cm (1610–1800 AD) seen in other variables do not rise above average level in Hill's N2. The represented species evenness rather displays a weak decrease through the whole assemblage. A common feature for all indexes is a distinct decrease towards present above 5 cm (1850 AD).

5.5.3. Correlation coefficients

There is a strong positive correlation between the Norwegian chironomid inferred temperature series and primary PCA axis ($r_s = 0.87$, $p < 0.001$). Spearman's correlation coefficient shows negative correlation between the Canadian inferred temperature and PCA axis 1 ($r_s = -0.64$, $p < 0.001$). PCA axis 1 and relative abundance of *Heterotrissocladius maeaeri*-type reach an almost perfect correlation ($r_s = 0.99$, $p < 0.001$). PCA axis 2 is correlated with the relative abundance of *Microspectra radialis*-type ($r_s = 0.55$, $p < 0.001$) and weakly correlated with the Canadian temperature reconstruction ($r_s = 0.22$, $p = 0.08$). Also LOI has weak positive correlation with PCA axis 2 ($r_s = 0.29$, $p = 0.36$) but a negative correlation with PCA axis 1 ($r_s = -0.26$, $p = 0.056$).

Diversity indexes are negatively correlated with the temperature reconstructions. Highest correlation is between Shannon H-index and the reconstruction based on the Norwegian training set ($r_s = -0.83$, $p < 0.001$), but the reconstruction correlates moderately also with species richness ($r_s = -0.49$, $p < 0.001$) and Hill's N2 ($r_s = -0.44$, $p < 0.001$).

Chlorophyll *a* derived productivity has a significant negative correlation with LOI ($r_s = -0.69$, $p < 0.001$) and of the PCA axis highest correlation occurs with component 1, although connection does not appear very strong ($r_s = 0.38$, $p = 0.004$). There is also some correlation between chlorophyll *a* reflectance and the Norwegian temperature model ($r_s = 0.29$, $p = 0.035$). Magnetic susceptibility has barely any correlation with other variables.

5.5.4. Temperature models

Since no previous paleoenvironmental chironomid studies have been carried out on Bjørnøya, representativeness of modern analogues with available training sets has to be carefully assessed. For this reason two different approaches were tested on the data a Norwegian training set (S. Brooks) and a North-Eastern Canadian training set (D. Francis).

The reconstructed temperatures based on the Norwegian training set range roughly between 8 and 11 °C (Fig. 20.), showing a relatively constant trend from the bottom to about 18 cm depth where a gradual cooling starts peaking at 8 cm. From since the trend has been warming until present. The best likelihood (29.4 %) and descriptive statistics of the WA-PLS model were met with component 2, yielding root mean square error of prediction (RMSEP) of 1.1 °C and jacknived correlation (r^2) of 0.90. In 91 % of the samples from Ellasjøen 95 % of the taxa is present in the training set, for all samples at least 80 %. Distance to closest modern analogue in the training set was analysed for each sample and only 10 (16 %) of the samples had good modern analogues with the cut-off chord distance less than the 90 % confidence interval of the mean minimum dissimilarity coefficient of the training set. Furthermore, 46 samples (72 %) have very poor modern analogues with chord distance over the 80 % confidence interval. Most of the good-analogue samples are close to the surface.

Different results were derived with the North-Eastern Canadian training set. The temperatures fluctuate within a range of 7.6–9.3 °C and rapid extreme swings occur frequently above 40 cm (1420 AD), while the reconstruction shows very uniform, trendless values from the bottom to approximately 18 cm depth, where a clear warming trend originates (Fig. 20.). Of taxa in Ellasjøen 95 % is the same as in the training set, however lower taxonomic resolution increases the similarity and may be misleading. This WA-model yields a RMSEP of 1.69 °C and bootstrapped r^2 of 0.88.

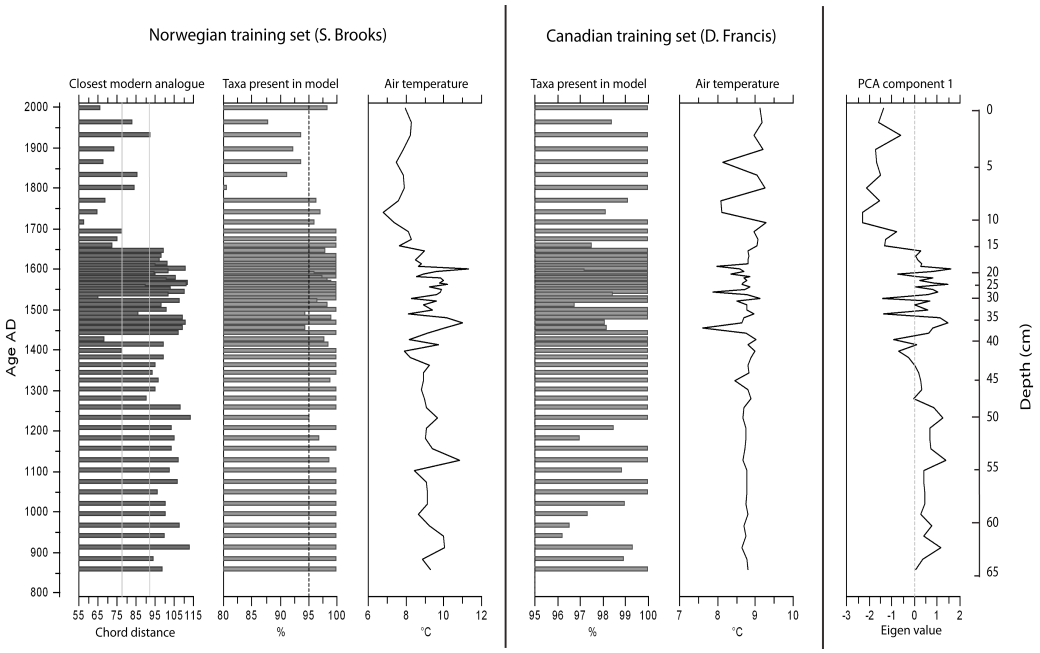

Figure 20. The chironomid based temperature reconstructions and percentage of common taxa with the Ellasjøen assemblage (cut off-value 95 % presented), respective to each training set approach. For Norwegian training set also the distance to closest modern analogue (MAT) is displayed with 90 % (77.5) and 80 % (92.5) confidence intervals (grey lines). PCA component 1 is displayed for temperature association reference.

6. DISCUSSION

6.1. Methods and reliability of results

During retrieval, sampling and laboratory analyses of sediment material much care was taken to minimize the errors and produce as accurate data as possible. In general the proxy results show coherent, good agreement with each other and are thus considered reliable. However, some aspects of the study require a more thorough investigation and are discussed below.

6.1.1. Chronology

As good age control is crucial for the interpretation, the chronology needs to be carefully assessed. 8 out of 10 ^{14}C samples show a chronological order, while specimens Ua-47864 and Ua-47865 displaying considerably older ages are considered as outliers (Table 3.). The finely laminated appearance of the core at this interval does not show

signs of re-sedimentation (Fig. 8.). Three possible factors as cause for the old age anomalies of Ua-47864 and Ua-47865 are considered. Firstly, both samples are moss specimens, thus longevity may become a problem as the life span of a single stem may cover surprisingly long time with slow growing rates in the arctic conditions (During 1979, Jónsdóttir et al. 2000). Secondly, in-washing of old organic material from the catchment area by for example snowmelt floods is also a possible way of redistributing older macrofossils from the catchment, documented as a common dating problem in the Arctic (Wolfe et al. 2004, Oswald et al. 2005). Slow decomposing of organic material in cold Arctic conditions allows dead plant remains to lie on the catchment area for extended periods of time. Sample Ua-47864 was picked from a horizon very rich in moss remains, which could represent an event of extreme inflow. Thirdly the dated material in sample Ua-47864 was a mixture of two moss species: *Philonotis caespitosa* and *Callioergon sp*., of which *Callioergon* is semi-aquatic, capable of living also under water and might hence preserve hard water signature in the carbon composition.

For the ^{210}Pb method good quality sediment density data is essential, and errors in this may compromise the dating results (Appleby 2001). During the storage and sub sampling water content may have changed, which creates random error to the density data. The series dated included both field extruded and core samples, serving as a source of further heterogeneity in the density data. Another possible error source is bioaccumulation of radionuclides that would disturb the natural air-borne concentrations. High concentrations of radionuclides, including ^{238}U decay chain (^{210}Pb) and ^{137}Cs have been shown to accumulate to seabirds and soils below seabird colonies (Gwynn et al. 2004, Dowdall et al. 2005), although it has also been argued that this shouldn't affect ^{210}Pb chronologies (Michelutti et al. 2008). The impact of seabirds on accumulation of heavy metals and persistent pollutants is however exceptionally high in Ellasjøen (Evenset et al. 2004, 2005, 2007a, 2007b). Also catchment processes and non-constant rate of accumulation due to variation in precipitation, spring floods or snow and ice cover may contribute to the complexity of the pattern (Appleby 2001, 2004).

^{210}Pb dates were considered and decided not to include to the model due to the large discrepancy between the different chronologies, which, if combined, would result in a malfunctioning model, and if only ^{210}Pb dates were applied, chronology of the lower

core would remain a mystery. The surface dates were put to context with previous ^{210}Pb chronology from Ellasjøen (Evenset et al. 2007b) which strongly disagree, but is in better agreement with the ^{14}C chronology. Surface chronology was also assessed against the rescaled temperature reconstruction, which suggests a very unlikely pattern in disagreement with general understanding of climate development. These incentives support the decision of further deciphering the ^{210}Pb model and relying on the radiocarbon based model. The results of spectrocolorimetry can be seen to support the decreased sedimentation rate towards the present day suggested by the radiocarbon model, as the sediment is increasingly dominated by algal primary productivity in the Q7/4 diagram (Fig. 11.). While chlorophyll *a* signal is also lower compared within core (Fig. 12.), dominance of primary production in sedimentary components could indicate low minerogenic input. Considering the habitus of immediate catchment area and draining systems such an increase in sedimentation rates assumed by the ^{210}Pb chronology seems unlikely. However, the chronology may be controversial and subject to further changes.

6.1.2. Temperature reconstructions and validation

Both the inferred air temperature models give modern values around 8–9 °C. This is about 2 °C higher than the instrumental record shows. Mean July and all over summer temperatures show a very constant, nearly trendless fluctuation with little variation around 3–5 °C in the instrumental record (Fig. 2.).

There are a few possible reasons why chironomid-inferred temperatures appear warmer than instrumental measurements. lake Ellasjøen is a productive arctic lake due to the high nutrient input via bird guano. Chironomids are sensitive to the trophic status of the environment and species adapted better to warmer conditions have a tendency to inhabit more nutrient rich lakes while cold-adapted species prefer oligotrophic conditions (Luoto 2011). Results from other harsh areas like Arctic Canada (Michelutti et al. 2011), western Spitsbergen (Brooks and Birks 2004, Luoto et al. 2014b), Nordaustlandet (Luoto et al. 2014a) and Antarctica (Izaguirre et al. 2003) show that bird influence can

have a great effect on lake ecology in means of increased faunal and floral diversity and productivity.

Other causes lie within the modelling and modern analogue problem. Most lakes included in a modern training set are frequently located in the vicinity of the centre of the environmental gradients, including temperature. Hence the training set is less representative and may yield less reliable results towards the extremes of the temperature gradient. When working in the very cold end of the spectrum, inferred temperatures are often overestimated due to the WA-based modelling approach which tends to draw the results towards the centre (Birks 1998). This is called the edge-effect and it is a common problem in extreme environments such as the Arctic. Velle et al. (2011) suggested that trimming the existing training sets could be a helpful tool in solving the problem of edge-effect. However, trimming did not affect the reconstructed temperature range in Velle et al. (2011), instead the trends underwent remarkable changes. This approach has not drawn much attraction in the paleolimnology community and is therefore not applied.

Another reason is lack of modern analogues in the training set. As seen from the modern analogue analysis of the Norwegian training set (Fig. 20.), the samples that reach a good resemblance are few (16 %). This may well be the major problem with Norwegian training set approach. Some of the lakes from Svalbard included in the training set are described by Brooks and Birks (2004) and the assemblage of these shallow ponds is quite different to the Ellasjøen profundal assemblage, which may partly explain the poor analogue conditions. Even if the modern analogues are poor, the Ellasjøen assemblage has a considerable amount of common taxa with both training sets, thus the within training set relations between speciestypes may still be representative and correctly reflect the environmental change in the Ellasjøen assemblage. With the Canadian training set the common taxa percentage is anomalously high due to lower taxonomic resolution, which reduces the reliability of this evaluation method.

The two reconstructions show almost opposite climate development, which pinpoints the importance of inference model assessment and evaluation. While the Norwegian model shows a cooler period above 18 cm depth, the Canadian model indicates

warming, also the concurrent major wiggles show divergent orientation. This is most likely due to different clustering of taxa within the models. While especially cold adapted members of the tribe Tanytarsini are present in the Ellasjøen assemblage, the tribe more commonly features species adapted to warmer conditions. In the Canadian approach all Tanytarsini were clustered in one causing the high presence of cold-adapted Tanytarsini to give an anomalous warmth signal. Interestingly, towards present, above 13 cm (1650 AD), the wiggles show parallel orientation in both models, clearly pinpointing the distinct cold period around (1760 AD) and agreeing on a cool event around 1850 AD. This highlights the difference of faunal assemblage between the top and the lower parts of the core, yet the reason for different model performance remains unclear.

Regardless of the overestimation of temperatures and poor-analogue conditions, the assemblage still seems to be well representative of temperature change. Both models pick out a period of instability (ca. 1400–1800 AD) and the different composition of faunal assemblage above 13 cm (1650- AD. The PCA analysis serves as an invaluable tool on model validation, showing a strong, unambiguous relationship between the chironomid assemblage and PCA component 1 (79 % of variance), which again is strongly correlated to the temperature reconstructions. The Norwegian training set model shows higher correlation ($r_s = 0.87$) than the Canadian ($r_s = -0.64$). PCA analysis gives a solid basis for use of the Norwegian approach in further interpretation and sufficiently validates the relative temperature change in it.

6.2. Sedimentary and ecological features

The sedimentary sequence features considerable amount of variability as revealed by the physical proxies, reflecting the natural changes within the lake and the catchment area. The catchment input seems to be strongly coupled with climatic variation, however, the carbonate bedrock surrounding the lake seems to have surprisingly little influence on the sediment. The fairly homogenic spectrocolorimetry signature indicates that there have not been large shifts on the source area of the sediment, but the proxy fluctuations are more likely reflecting changes in amount of inflow, lake level and amount of organic production. Identified sedimentary units relate well to the

differencies in above mentioned variability and interrelatedly describe the climate-induced changes in the lake-catchment system: stable conditions (unit 1), followed by increasing (unit 2) and extreme (unit 3) inflow and sedimentation rate, again leading to more stable conditions again (unit 4).

Intervals of high inflow and rapid sedimentation (up to 2 mm/year) occuring between 1200 and 1700 AD are represented as increased minerogenic content depicted by magnetic susceptibility trends and iron reflectance with lower (diluted) chlorophyll *a* signature. LOI shows varied fluctuation during these events, and disagreement with the primary production signal may indicate increased allochthonous input of organic matter. Catchment area, where not dominated by bedrock exposure, composes of permafrost soils, where active layer detachment processes are reinforced by higher summer temperature, early spring thaw and higher summer-autumn precipitation (French 2007). Variation of the organic components is perceivable also in spectrocolorimetric signature and would be an interesting topic for further research.

A series of white layers is a distinct feature of the sediment series, and all except for one (54 cm, 1120 AD) occur during the high-inflow interval described above. They appear slightly coarser, specifically low in organic remains and have a fine normal grading (Katja Baum, personal communication, 2014). This suggests that these marker horizons are rapid sedimentation event layers. All white layers (54, 49.5, 30 and 26.5 cm) and the moss rich layer (43.5 cm) occur after a rapid swing from cold to warm according to the chironomid inferred temperatures. Possible set off mechanisms may thus be of climatic origin, related to the response of periglacial catchment processes to the increased warmth and/or precipitation.

After 1700 AD the sedimentation rate has gradually decreased being considerably lower since about 1800 AD. Sediment is characterised by decreasing magnetic susceptibility, low iron reflectance, increasing LOI and water content and low but steady chlorophyll *a* signal, as well as lower inferred temperature. This might reflect a lowering lake level after the high temperature and precipitation period, with reduced fluvial (minerogenic) input and steady conditions. Increasing LOI and steady primary production signal would favour a shallower setting, as high allochthonous input is unlikely with low

sedimentation rate. A photograph in Horn and Orvin (1928, Plate VII A.) seems to show a slightly higher lake level, possibly related to the paleoshoreline marked in Figure 7.A). Paleoshorelines on at least two levels were observed around the lake supporting substantial fluctuations of lake level in the past.

The ecology in lake Ellasjøen, chironomid assemblage and chlorophyll *a* derived primary production, seems to reflect the temperature trends well. Through the studied series, the lake system is evolving towards higher dominance of primary production in the sediment composition as seen in the Q7/4 diagram (Fig. 11.). This trend can be seen to continue and enforce towards the surface in core ESGC3-13, where reflectance was measured through the whole core length (Katja Baum, personal communication, 2014). In the uppermost 1 cm of ESGC3-13, the organic reflectance is the dominant signal outpacing the iron reflectance. This could reflect change of the climate towards more favourable or related increase of nutrient input from seabirds visiting the lake (Luoto et al. 2014a, 2014b).

The chironomid population of lake Ellasjøen composes of species typical to cold, arctic lakes (Brooks et al. 2007). While Ellasjøen is a relatively productive and nutrient rich arctic lake, higher chironomid abundance could have been expected. Higher sedimentation rate and lower density towards the surface leads to dilution of head capsule concentration and the extensive population of arctic char (*Salvelinus alpinus*) in the lake (Klemetsen et al. 1985) may put strain on the chironomid population. Diversity of the the chironomids is fluctuating, but the diversity indexes clearly indicate that the assemblage is dominated by few taxa. The pattern of the diversity indexes and the prominent decrease in diversity towards present since 1850 AD implies that the ecology was more diverse during the cold phases of LIA. High negative correlation (Shannon: r_s = -0.83) between diversity indexes and the temperature reconstruction imply, that diversity is driven by climatic variables. The temperature optimums of the taxa in Ellasjøen seem to be lower than present conditions, and if the recent warming trend depicted by the instrumental record and primary production continues or enforces, the effects on Ellasjøen chironomid population might be drastic.

6.3. Climate development of Bjørnøya

6.3.1. Medieval Warm Period and increasing variability (850–1350 AD)

The oldest part of the core (ca. 850–1150 AD) reveals over all very little changes in any of the studied parameters, indicating fairly stable conditions. The time period is generally associated with the Medieval Warm Period (MWP) in Western Europe, when mild climate conditions for example spurred the Norse settling in Iceland (Axford et al. 2009) and Greenland (D'Andrea et al. 2011). However, temperatures feature high regional differences related to the North Atlantic Oscillation (NAO) and no spatially coherent distinctly warm period has been defined (Bradley et al. 2003b, D'Arrigo et al. 2006). Although persistently positive PCA component 1 scores reflect warm and fairly steady temperature association, Ellasjøen chironomid assemblage does not indicate particularly elevated temperatures (Fig. 20.). This could be due to the large maritime component in the climate of the island. Dylmer et al. (2013) report dominance of Arctic surface water in the western Barents Sea (WBS) at this time, which contributes to cooler conditions. Furthermore, MWP warmth is often modest in arctic reconstructions (Kaufman et al. 2009, Miller et al. 2010), though detectable (McKay and Kaufman 2014). Stable conditions are likely related to persistent positive winter NAO signal which was exceptionally dominant during the MWP (Trouet et al. 2009). NAO^+ signal causes milder and wetter conditions in northern Europe and areas along the North Atlantic current. NAO also has a great effect on ecosystems with a positive response to biomass in aquatic ecosystems and earlier timing of life events associated with high NAO^+ index (Blenckner and Hillebrand 2002). The abundance of chironomids in Ellasjøen is highest during this interval and starts to decline after the NAO index turns negative at 1350–1400 AD (Fig. 15).

At ca. 1150–1200 AD the quality of sediment changes from fairly dense to softer and less uniform. This marks a starting point of a gradually increasing sedimentation rate. Dylmer et al. (2013) suggests that due to the continuous strengthening of North Atlantic Current the Atlantic water started to dominate in the WBS around the same time, which would result in increase of warmth and moisture transport towards Bjørnøya. This could increase inflow to the lake and thus increase sedimentation rate. Accompanied with the

higher sedimentation rate, the sporadic occurrence of white layers is introduced to the sediment series, which further supports increased catchment input and instability.

6.3.2. The Little Ice Age (1350-1850 AD)

At 1350 - 1750 AD a period of climatic instability and colder conditions towards the end is represented in the Ellasjøen sedimentary record and interpreted as the Little Ice Age (LIA) (Fig. 20). As defining the LIA divides opinions, should it be referred to as the cold climate anomaly evident in many temperature records ("LIA climate") or the longer period detected from glacial advances ("LIA glacierization") (Matthews and Briffa 2005), herein the whole period associated with climatic instability starting around 1350 AD is treated as LIA and the severe climate conditions at the 17th to 18th century are referred to as the culmination or peak of LIA.

The sedimentation rate during LIA is high, 0.6–2 mm/year. In the gravity core ESGC9-13, dipping layers occur below ~15 cm depth suggesting former strong fluvial input from NE. Temporal context of ESGC9-13 is unsolved, but correlation with ESGC1-13 based on distinct white layer suggests that horizontal deposition started during 17th century. As the setting of Bjørnøya is tectonically stable such a drastic change in erosion rates is most likely climate-induced. The causes of LIA are not fully resolved, but a combination of decreased solar irradiance, increased volcanic activity and changes in the ocean-atmosphere circulation patterns in the North Atlantic have been suggested (Wanner et al. 2011). The Maunder Minimum in amount of sunspots and increase of volcanic aerosoles coincide with the culmination of Little Ice Age (Crowley 2000).

Glacier evidence indicate that LIA initiated some time in the thirteenth or fourteenth century in the North Atlantic Region, but due to the spatially heterogenic evidence, it is considered a non-synchronous cold period with high regional variability (Grove 2001). In the Ellasjøen record a drop in temperatures associated with the onset of LIA occurs at ca. 1360–1400 AD, while most of the LIA period on Bjørnøya does not appear particularly cold, rather the opposite (Fig. 20.). Dylmer et al. (2013) point out the

dominance of Atlantic water in the WBS surface waters, which favours milder conditions.

Soon after initiation of LIA a two peaked (1410 and 1460 AD) fairly warm period takes place in the Ellasjøen record (Fig. 20.). Helama et al. (2009) reports such a mid-LIA transient warmth at 1391-1440 AD in an annually resolved dendrochronological record from northern Fennoscandia. A similar brief warm event can also be traced from high resolution reconstructions from Svalbard at ca. 1400–1440 AD, both in summer (D'Andrea et al. 2012) and winter (Divine et al. 2011) temperatures. Such a widely traceable event may be related to a pulse in increasing flow of Atlantic water and can be seen in marine records at WBS and Vøring plateau in Dylmer et al. (2013) .

The LIA series from Ellasjøen features comparatively high variability in temperatures at 1350–1650 AD (Fig. 20.) Presented difference in variability may partly be anomalous due to higher sedimentation rate induced increased resolution; yet can be seen to suggest climatic instability. The onset of LIA is associated with a shift from positive to negative NAO phase (e.g. Visbeck et al. 2003, Olsen et al. 2012, Dylmer et al. 2013). NAO^- phases appear as more variable and instable in the Northern Atlantic than positive NAO phases, which may partly explain the shifting climate conditions during LIA. NAO index is also positively correlated with sea ice extent with most pronounced effect in the eastern North Atlantic (Vinje 2001).

Helama et al. (2009) finds the variability patterns to be of inter-annual scale during LIA, while during MWP cycles were of multi-decadal (50–60 years) scale, supporting more heterogeneous climate during LIA and suggests the oceanic circulation to be a major influence in the climate. Dylmer et al. (2013) state that despite the dominance of Atlantic waters, the ocean around Bjørnøya is also influenced by westward flow of Arctic water through the Bear Island Current, and may thus have been a subject to highly fluctuating sea ice conditions and strong seasonal gradients, characterized by early spring break up of the sea ice and Atlantic water dominance during the summer, hence supporting increased seasonality.

The mechanisms affecting the seasonality at Bjørnøya could compose of dominant NAO^- index related larger extent of sea ice, which can cause isolation of the oceanic heat transport system from the atmosphere, resulting in colder winter temperatures. Coupled with steady increase in Atlantic water flow, increased winter precipitation (mainly snow) would further build up the sea-ice, whereas spring precipitation (rain) accompanied with the warming air temperature due to increasing solar heating after the polar night would contribute to the early break up of the sea ice, in addition to sub-surface melting effect of Atlantic water. Early spring break up of sea ice would allow a longer growing season and the dominance of Atlantic water input during summer, thus explaining the generally high reconstructed temperatures, and increased summer precipitation would lead to higher sedimentation rate.

For the 15th and 16th century temperature reconstruction suggest decadal to multidecadal cyclicity and warming conditions (Fig. 20.). This time also features again a more positive NAO index (Olsen et al. 2012). The sedimentation rate was especially high ca. 1550–1600 AD. According to the Q7/4 diagram (Fig. 11.) the sedimentation during this period was clearly more minerogenic and less organic suggesting increased inflow from the catchment. This correlates well with a significant increase in the flow of Atlantic water recorded in the Fram Strait and in the WBS (Dylmer et al. 2013).

A gradual decrease in temperatures at Ellasjøen started about 1600 AD, and is accompanied by a concurrent, evident decrease in chlorophyll *a* derived primary production (Figures 20. and 12.). A distinct cold peak is observed at ca. 1740 AD, interpreted as the culmination of the LIA, which is followed by a rising temperature trend holding to the present. The decreasing trend and culmination of LIA could be associated with more persistent sea ice conditions, and the culmination also coincides with the Maunder minimum. A 400 year sea ice extent reconstruction from Svalbard based on historical records and log books indicate that atleast between 1630 and 1660 the edge of open water in August has had a very southern location around 76° N (Vinje 1998).

The temperature drop at the peak of LIA is 1-2 °C colder than present and 2 °C colder than the average of reconstructed temperature series. Similar timing for the LIA peak

(between 1550–1850 AD) has been presented in the Arctic composite climate reconstructions (Bradley et al. 2003a, Mann and Jones 2003, Moberg et al. 2005, Kaufman et al. 2009). While the intensity varies across the Arctic, it seems to be most pronounced in the North Atlantic sector (Miller et al. 2010). Climate reconstructions from a transect along the North Atlantic indicate that the magnitude of the summer temperature changes associated with culmination of LIA are in the range of <1 to 2 °C. The LIA at it's peak was for example approximately 2 °C cooler in Finland (Luoto 2013), 1.5 °C cooler in Lapland (Helama et al. 2009) and in Iceland (Axford et al. 2009), and 1-2 °C colder in Greenland (Axford et al. 2013), compared to modern values.

The peak of LIA correlates with the GISP2 ice core record from Greenland, where lowest associated temperatures occurred between 1579 and 1730 AD, especially 1680–1730 AD (Kreutz et al. 1997). The Icelandic historical records and ice core isotope data from Greenland are in agreement with each other, but seem to show some discrepancy in phasing compared with the European records (Turner and Marshall 2011). This is probably related to the NAO and the seesaw pattern of the North Atlantic current, which indicates cooler conditions in Iceland and southern Greenland while northern Europe is warm and the opposite (Miettinen et al. 2011). Pattern is due to relative strength of the Irminger current branching westwards south of Iceland and the North Atlantic Current continuing north along the coast of Norway.

High-resolution summer temperature reconstructions from the Atlantic Arctic are especially rare. However, a recent study from Svalbard shows a similar patter with LIA of unprecedented warmth featuring increasing variability from ca. 1400 to 1700 AD, with extreme variability during the 17th century (D'Andrea et al. 2012). The coldest extreme value is recorded at about 1630 AD, with rapid swings soon after transforming to a coherent increasing temperature development.

Other records from Svalbard do not show a pattern as evident. The Little Ice Age in Svalbard has been traced by glacial advances, which generally feature their greatest neoglacial extents as young as 20th century (Mangerud and Landvik 2007). Lacustrine studies show increased glacial activity also around 1300 AD (Svendsen and Mangerud

1997). Velle et al. (2011) concludes that the two-phased LIA is represented in Skardtjørna chironomid assemblage at 1200 AD and 1700–1800 AD. Inferred temperature change is <1 °C. Also Brooks and Birks (2004) suggest a climate induced environmental change caused faunal changes in two lakes in Spitsbergen at about 200 calender years ago, and possibly in one lake 500 years ago.

The end of LIA in Ellasjøen record is difficult to assess, as the temperature does not rise back to even the average of the series. However, the chironomid assemblage features clearly higher diversity at 1600–1850 AD during the cold phases of LIA (Fig. 19.). The distinct decrease starting at 1850 AD may thus be interpreted as the end of LIA.

6.3.3. From LIA to present (1850–2013 AD)

General Arctic temperature development since the LIA has been dominated by a persistent warming trend, interrupted by a few colder periods, and is considered to accelerate towards the end of the 20th century (Overpeck et al. 1997, Kaufman et al. 2009, Miller et al. 2010, Førland et al. 2011). The trend in Ellasjøen temperature record is warming, although in modest scale. From 1740 AD the temperature has risen almost 2 °C but has not exceeded the warmth prior to the culmination of LIA. (Fig. 20.) This pattern is different to other terrestrial (Holmgren et al. 2010, D'Andrea et al. 2012) and marine (Spielhagen et al. 2011, Dylmer et al. 2013) records in Svalbard as well as arctic composite reconstructions (Overpeck et al. 1997, Mann and Jones 2003, Kaufman et al. 2009, Miller et al. 2010, McKay and Kaufman 2014) which frequently display a distinct warming peak at present. However, depicting such a recent change may suffer from the slow sedimentation rate during the past century. Instrumental record on Bjørnøya shows a warming trend of 0.08 °C per decade in summer temperatures through the 20th century (1920–2011), and 0.39 °C at 1975–2011 (Førland et al. 2011). However, the summer temperature trend was cooling between 1943 and 1988, which may explain the cooling seen in the modern sample of lake Ellasjøen. The accelerated warming has taken place on Bjørnøya during only the past 10–15 years according to the instrumental record (Fig. 2.), being most distinct in winter (DJF) temperatures and statistically insignificant in summer temperatures (Førland et al. 2011). As chironomids reflect primarily the summer temperature (Eggermont and Heiri 2012), results support the instrumental data.

Since the LIA winter NAO has fluctuated on a decadal level (Luterbacher et al. 2002). The cold periods experienced since the LIA are associated with negative NAO phases. The latest NAO^- event was in the 1960's (Hurrell 1995), featuring the coldest period of arctic instrumental records (Førland and Hanssen-Bauer 2002). This is evident also in the Bjørnøya instrumental record (Fig. 2.). In the 1960's along with the colder averages the temperature is also highly variable, particularly in the mid-winter (DJF) compared to for example the 1930's, which was a period of strongly positive NAO and recorded as the warmest decade in the Arctic until the 2nd millennium (Førland et al. 2011). Thus the meteorological record supports the suggested general pattern of increased climate variability in seasonal components on Bjørnøya during NAO^- phases. Since the 1960's high NAO^+ signal has been especially persistent possibly due to north-eastward shifting of NAO (Cassou et al. 2004) and is, accompanied with associated ocean-ice-atmosphere interactions, one of the main contributors to the generally observed increasing temperatures and increasing precipitation in the Norwegian Arctic (Hanssen-Bauer and Førland 1998).

The present warming is strongly connected to excess flow of AW to the north and is evident in records from Fram Strait (Spielhagen et al. 2011, Dylmer et al. 2013) and western Svalbard (D'Andrea et al. 2012), where the effect is especially pronounced due to positive feedback mechanisms connected with reducing sea ice cover and related increasing effect of Atlantic water. Further south this change is not as distinct due to lack of sea ice feedback processes and thus reduced polar amplification. In WBS the dominance of Atlantic water has started about a 1000 years ago, while in the Fram Strait this didn't happen until the 20th century (Dylmer et al. 2013). Furthermore, even if the Atlantic waters dominate the WBS, it is also influenced by westward flowing polar waters and the location of Arctic Front crosses the WBS in the vicinity of Bjørnøya. Dylmer et al. (2013) presents warming sea surface waters during the past century from WBS, but the magnitude does not outpace earlier warm periods. Oceanic and atmospheric heat transport is the major source of warmth on Bjørnøya and the extensive fogginess may reduce the importance of direct solar heating.

In the long-term context, temperature record from Ellasjøen features a signal very different to the state-of-the-art Arctic composite reconstructions. Kaufman et al. (2009)

and PAGES 2k Consortium (2013), for example, depict a cooling trend in temperatures over the past 2000 years, culminating as the LIA and a very distinct twentieth century warming. There is no evidence of long-term cooling or accelerated modern warming in Ellasjøen series. Also a study from western Spitsbergen (D'Andrea et al. 2012) presents a summer temperature record where no long-term cooling is visible, yet modern warming is very prominent. The full training set version of chironomid-inferred summer temperature reconstructions by Velle et al. (2011) does not show any cooling either, rather warming until about 1600 AD followed by cooling.

Furthermore, a winter temperature reconstruction from Svalbard based on oxygen isotopes in ice cores (Divine et al. 2011) shows a prominent cooling trend followed by recent warming. These results suggest that the long-term cooling is not present or evident in the Norwegian Arctic summer temperatures during the past 2000 years, but is well reflected in the winter temperatures. Compared records are fairly short which can hinder depicting long-term trends, however, only ice core (i.e. winter temperature) data from Svalbard is included in the composite models, hence the seasonal variation in Svalbard is unrepresented in the models regardless. Analysis of present instrumental data from Svalbard reveals winter temperature variation higher than summer variation, in the scale of approximately 2 °C and 10 °C respectively (Førland and Hanssen-Bauer 2003), further highlighting the importance of intra-annual variability.

The long-term context of seasonal components in Arctic climate is poorly understood, hence the results and recent research imply importance of building a more complete picture of seasonal and annual temperature variability in the Arctic. Bjørnøya serves as a good example to highlight also the importance of locally solved arctic climate records to better understand the spatial variability in climate dynamics and their connections to the larger systems when assessing past and future climate development.

7. CONCLUSIONS

The variation in physical and ecological features determined from lake Ellasjøen sedimentary series shows that the lake is sensitive to environmental change and the climatic variability of past is detectably archived in the sediments. With reservation considering the chronology, following concluding remarks can be drawn.

The general climate development of Bjørnøya features modest warmth during MWP (850–1150 AD, high variability during LIA (1350–1850 AD) and a slowly rising trend towards the present. The dominant drivers in long-term temperature development on Bjørnøya seem to be the NAO, interaction of warm Atlantic water and cold polar water in the WBS and related sea ice extent, underlining the coupling relationships within ice-ocean-atmosphere interaction.

A clear deviation from the generally accepted climate history of the Arctic is lack of long-term cooling, peaking as the LIA. Reconstructed temperatures support recent data from Svalbard and suggest increased seasonality during LIA, related to the interaction of cold and warm water masses and respective sea ice dynamics. Triggers behind the deteriorating conditions leading to the culmination of LIA are difficult to identify, but conditions are likely related to increased sea-ice extent and polar water circulation around Bjørnøya.

The rising temperature development after LIA remains modest and no present warming can be depicted, in contrast to composite records of the Arctic. The instrumental data from Bjørnøya supports little change in summer temperatures, and regardless the low resolution at the top hampering the interpretation, the main causes are suggested to be 1) the reduced polar amplification due to earlier introduction of Atlantic water (11th instead of 20th century) and related sea ice patterns, and 2) the interaction of warm and cold ocean currents contributing to the maritime climate of Bjørnøya, where present day seasonality is lower than in e.g. Spitsbergen.

These findings indicate that the seasonal component in Arctic climate may play a significant role, which highlights the need of regionally solved high-resolution records

in order to comprehensively understand the dynamics and interrelationships of underlying driving factors of Arctic climate in order to improve basis for future climate assessments.

Overall, the results of this study support recent results from the surrounding areas, proving that Bjørnøya is a climatically sensitive key site linking the northern Fennoscandia and Svalbard together along the heat and moisture transport mechanisms of the northern seas.

8. ACKNOWLEDGEMENTS

This master's project, despite a few desperate moments, has been a thrilling adventure that would never have been possible without the contributions of others. I sincerely wish to thank my supervisors Tomi Luoto and Anne Hormes for gently teaching, guiding and encouraging me through the process. I am especially grateful to Anne for financially and logistically making this project possible under HolS (Holocene environmental change on Svalbard - multiproxy climate reconstructions from lake sediments), and for sending me to the AAW 2014. I can't thank enough our amazing field party, Anne, William D'Andrea, Willem van der Bilt, Torgeir Røthe, Katja Baum and Alex Hovland, for collecting excellent samples in tricky conditions and keeping up the great spirit despite all the grey, fog, wind and bird carcasses!

I would like to express my gratitude to Steve Brooks and Donna Francis for kindly creating the chironomid inferred temperature reconstructions, and Johannes Enroth for identifying the macrofossil samples for radiocarbon analysis. I thank Maxime Debret for help with everything that relates to spectrocolorimetry, from lab to figures. I would like to acknowledge Eva Sessford for excellent reconnaissance mapping.

Line Nicolaisen and Katja Baum, I truly enjoyed working with you on our respective cores and thank you for all the support, sharing, discussions and what not! I sincerely thank Professor Veli-Pekka Salonen for comments, and especially for being a source of inspiration for my Arctic interests that eventually led me to UNIS. Family and friends,

your continuous support has made my day so many times during this process that I lost the count long time ago, thank you!

Financial support for this project was granted by Suomen Hyönteistieteellinen Seura (Finnish entomologic society) and Department of geosciences and geography, University of Helsinki.

9. REFERENCES

ACIA (Arctic Climate Impact Assessment). 2004. Impacts of a warming Arctic: Arctic climate impact assessment, Cambridge University Press, Cambridge. 139 p.

Andersen, F. S. 1938. Spätglaciale Chironomiden. Meddelelser fra Dansk Geologisk Forening, 9, 320–326.

Appleby, P. G. 2001. Chronostratigraphic techniques in recent sediments. In: Last, W. M. and Smol, J. P. (eds.) Tracking Environmental Change Using Lake Sediments. Volume 1: Basin analysis, Coring, and Chronological Techniques. Kluwer Academic Publishers. Dordrecht, The Netherlands. 171–203.

Appleby, P. G. 2004. Environmental change and atmospheric contamination on Svalbard: sediment chronology. Journal of Paleolimnology, 31, 433–443.

Appleby, P. G. 2008. Three decades of dating recent sediments by fallout radionuclides: a review. The Holocene, 18, 83–93.

Appleby, P. G. and Oldfield, F. 1978. The calculation of 210Pb dates assuming a constant rate of supply of unsupported 210Pb to the sediment. Catena, 5, 1–8.

Armitage, P., Cranston, P. S. and Pinder, L. C. V. (eds.) 1995. The Chironomidae. The biology and ecology of non-biting midges, Chapman and Hall, London. 572 p.

Axford, Y., Geirsdóttir, Á., Miller, G. H. and Langdon, P. G. 2009. Climate of the Little Ice Age and the past 2000 years in northeast Iceland inferred from chironomids and other lake sediment proxies. Journal of Paleolimnology, 41, 7–24.

Axford, Y., Losee, S., Briner, J. P., Francis, D. R., Langdon, P. G. and Walker, I. R. 2013. Holocene temperature history at the western Greenland Ice Sheet margin reconstructed from lake sediments. Quaternary Science Reviews, 59, 87–100.

Balsam, W. L., Damuth, J. E. and Schneider, R. R. 1997. Comparison of shipboard vs shore-based spectral data from Amazon Fan cores: implications for interpreting sediment composition. In: Flood, R. D., Piper, D. J. W., Klaus, A. and Peterson, L. C. (eds.) Proceedings of the Ocean Drilling Program, Scientific Results. Volume 155. 193–215.

Balsam, W. L., Deaton, B. C. and Damuth, J. E. 1998. The effects of water content on diffuse reflectance spectrophotometry studies of deep-sea sediment cores. Marine Geology, 149, 177–189.

Barnekow, L., Possnert, G. and Sandgren, P. 1998. AMS 14C chronologies of Holocene lake sediments in the Abisko area, northern Sweden – a comparison between dated bulk sediment and macrofossil samples. Geologiska föreningens i Stockholm förhandlingar, 120, 59–67.

Battarbee, R. W., Anderson, N. J., Bennion, H. and Simpson, G. L. 2012. Combining limnological and palaeolimnological data to disentangle the effects of nutrient pollution and climate change on lake ecosystems: problems and potential. Freshwater Biology, 57, 2091–2106.

Birks, H. H. and Birks, H. J. B. 2006. Multi-proxy studies in palaeolimnology. Vegetation history and Archaeobotany, 15, 235–251.

Birks, H. J. B. 1998. Numerical tools in palaeolimnology - Progress, potentialities, and problems. Journal of Paleolimnology, 20, 4.

Birks, H. J. B., Heiri, O., Seppä, H. and Bjune, A. E. 2010. Strengths and Weaknesses of Quantitative Climate Reconstructions Based on Late-Quaternary Biological Proxies. The Open Ecology Journal, 3, 68–110.

Blaauw, M. 2010. Methods and code for 'classical' age-modelling of radiocarbon sequences. Quaternary Geochronology, 5, 512–518.

Blenckner, T. and Hillebrand, H. 2002. North Atlantic Oscillation signatures in aquatic and terrestrial ecosystems—a meta-analysis. Global Change Biology, 8, 203–212.

Bradley, R. S., Briffa, K. R., Cole, J., Hughes, M. K. and Osborn, T. J. 2003a. The Climate of the Last Millennium. In: Alverson, K. D., Bradley, R. S. and Pedersen, R. S. (eds.) Paleoclimate, Global Change and the Future. Springer. Berlin. 105–141.

Bradley, R. S., Hughes, M. K. and Diaz, H. F. 2003b. Climate in Medieval Time. Science, 302, 404–405.

Brodersen, K. P. and Quinlan, R. 2006. Midges as palaeoindicators of lake productivity, eutrophication and hypolimnetic oxygen. Quaternary Science Reviews, 25, 1995–2012.

Brooks, S. J. 2006. Fossil midges (Diptera: Chironomidae) as palaeoclimatic indicators for the Eurasian region. Quaternary Science Reviews, 25, 1894–1910.

Brooks, S. J., Bennion, H. and Birks, H. J. B. 2001. Tracing lake trophic history with a chironomid–total phosphorus inference model. Freshwater Biology, 46, 513–533.

Brooks, S. J. and Birks, H. J. B. 2001. Chironomid-inferred air temperatures from Lateglacial and Holocene sites in north-west Europe: progress and problems. Quaternary Science Reviews, 20**,** 1723–1741.

Brooks, S. J. and Birks, H. J. B. 2004. The dynamics of Chironomidae (Insecta: Diptera) assemblages in response to environmental change during the past 700 years on Svalbard. Journal of Paleolimnology, 31, 483–498.

Brooks, S. J., Langdon, P. G. and Heiri, O. 2007. The identification and use of Palaeoarctic Chironomidae larvae in palaeoecology. QRA Technical Guide No. 10, Quaternary Research Association, London. 276 p.

Cassou, C., Terray, L., Hurrell, J. W. and Deser, C. 2004. North Atlantic Winter Climate Regimes: Spatial Asymmetry, Stationarity with Time, and Oceanic Forcing. Journal of Climate, 17, 1055–1068.

Chapman, M. R. and Shackleton, N. J. 1998. What level of resolution is attainable in a deep-sea core? Results of a spectrophotometer study. Paleoceanography, 13, 311–315.

Cohen, A. S. 2003. Paleolimnology: the history and evolution of lake systems, Oxford University Press, Inc., New York. 500 p.

Cohen, K., Finney, S. and Gibbard, P. 2013. International Chronostratigraphic Chart. 2013/1. International Commission on Stratigraphy, http://www.stratigraphy.org/ICSchart/ChronostratChart2013-01.pdf

Crowley, T. J. 2000. Causes of climate change over the past 1000 years. Science, 289, 270–277.

Dallmann, W. K. and Krasil'ščikov, A. A. (eds.) 1996. Geological map, of Svalbard 1 :50 000, sheet D20G Bjørnøya. Norsk Polarinstitutt Temakart nr. 27.

D'Andrea, W. J., Huang, Y., Fritz, S. C. and Anderson, N. J. 2011. Abrupt Holocene climate change as an important factor for human migration in West Greenland. Proceedings of the National Academy of Sciences of the United States of America, 108, 9765–9769.

D'Andrea, W. J., Vaillencourt, D. A., Balascio, N. L., Werner, A., Roof, S. R., Retelle, M. and Bradley, R. S. 2012. Mild Little Ice Age and unprecedented recent warmth in an 1800 year lake sediment record from Svalbard. Geology, 40, 1007–1010.

D'Arrigo, R., Wilson, R. and Jacoby, G. 2006. On the long-term context for late twentieth century warming. Journal of Geophysical Research, 111, D03103.

Dean, W. E. J. 1974. Determination of carbonate and organic matter in calcareous sediments and sedimentaery rocks by loss on ignition: comparison with other methods. Journal of Sedimentary Petrology, 44, 242–248.

Dearing, J. A. 1999. Environmental Magnetic Susceptibility. Using the Bartington MS2 System, Bartington Instruments Ltd, 54 p.

Debret, M., Sebag, D., Desmet, M., Balsam, W., Copard, Y., Mourier, B., Susperrigui, A.-S., Arnaud, F., Bentaleb, I., Chapron, E., Lallier-Vergès, E. and Winiarski, T. 2011. Spectrocolorimetric interpretation of sedimentary dynamics: The new "Q7/4 diagram". Earth-Science Reviews, 109, 1–19.

Divine, D., Isaksson, E., Martma, T., Meijer, H. A. J., Moore, J., Pohjola, V., Wal, R. S. W. v. d. and Godtliebsen, F. 2011. Thousand years of winter surface air temperature variations in Svalbard and northern Norway reconstructed from ice-core data. Polar Research, 30, 7379.

Dowdall, M., Gwynn, J. P., Gabrielsen, G. W. and Lind, B. 2005. Assessment of Elevated Radionuclide Levels in Soils Associated with an Avian Colony in a High Arctic Environment. Soil and Sediment Contamination, 14, 1–11.

During, H. J. 1979. Life strategies of Bryophytes: a preliminary review. Lindbergia, 5, 2–18.

Dylmer, C. V., Giraudeau, J., Eynaud, F., Husum, K. and Vernal, A. D. 2013. Northward advection of Atlantic water in the eastern Nordic Seas over the last 3000 yr. Climate of the Past, 9, 1505–1518.

Eggermont, H. and Heiri, O. 2012. The chironomid-temperature relationship: expression in nature and palaeoenvironmental implications. Biological Reviews, 87, 430–456.

eKlima. 2014. Weather- and climate data from Norwegian Meteorological Institute from historical data to real time observations Norwegian Meteorological Institute. http://www.eklima.met.no (Accessed 26.2.2014)

Engelskjøn, T. 1986. Eco-geographical relations of the Bjørnøya vascular flora, Svalbard. Polar Research, 5, 79–127.

Evenset, A., Carroll, J., Christensen, G. N., Kallenborn, R., Gregor, D. and Gabrielsen, G. W. 2007a. Seabird Guano Is an Efficient Conveyer of Persistent Organic Pollutants (POPs) to Arctic Lake Ecosystems. Environmental Science and Technology, 41, 1173–1179.

Evenset, A., Christensen, G. N., Carroll, J., Zaborska, A., Berger, U., Herzke, D. and Gregor, D. 2007b. Historical trends in persistent organic pollutants and metals recorded in sediment from Lake Ellasjøen, Bjørnøya, Norwegian Arctic. Environmental Pollution, 146, 196–205.

Evenset, A., Christensen, G. N. and Kallenborn, R. 2005. Selected chlorobornanes, polychlorinated naphthalenes and brominated flame retardants in Bjørnøya (Bear Island) freshwater biota. Environmental Pollution, 136, 419–430.

Evenset, A., Christensen, G. N., Skotvold, T., Fjeld, E., Schlabach, M., Wartena, E. and Gregor, D. 2004. A comparison of organic contaminants in two high Arctic lake ecosystems, Bjørnøya (Bear Island), Norway. The Science of the Total Environment, 318, 125–141.

Førland, E. J., Benestad, R., Hanssen-Bauer, I., Haugen, J. E. and Skaugen, T. E. 2011. Temperature and Precipitation Development at Svalbard 1900–2100. Advances in Meteorology, 2011, Article ID 893790, 14 p. DOI:10.1155/2011/893790

Førland, E. J. and Hanssen-Bauer, I. 2002. Climate variations and implications for precipitation types in the Norwegian Arctic. Klima, 24. Norwegian Meteorological Institute. 21 p.

Førland, E. J. and Hanssen-Bauer, I. 2003. Past and future climate variations in the Norwegian Arctic: overview and novel analyses. Polar Research, 22, 113–124.

Francis, D. R., Wolfe, A. P., Walker, I. R. and Miller, G. H. 2006. Interglacial and Holocene temperature reconstructions based on midge remains in sediments of two lakes from Baffin Island, Nunavut, Arctic Canada. Palaeogeography Palaeoclimatology Palaeoecology, 236, 107–124.

French, H. M. 2007. The Periglacial Environment, Third edition, John Wiley & Sons Ltd. Great Britain. 478 p.

Gabrielsen, R. H., Færseth, R. B., Jensen, L. N., Kalheim, J. E. and Riis, F. 1990. Structural elements of the Norwegian Continental Shelf. Part I: The Barents Sea region. Norwegian Petroleum Directorate, Bulletin, 6, 33 p.

Gannon, J. 1971. Two counting cells for the enumeration of zooplankton micro-crustacea. Transactions of the American Microscopical Society, 90, 486–490.

Grove, J. M. 2001. The initiation of the "Little Ice Age" in regions around the North Atlantic Climatic Change, 48, 53–82.

Gwynn, J. P., Dowdall, M., Davids, C., Selnæs, Ø. G. and Lind, B. 2004. The radiological environment of Svalbard. Polar Research, 23, 167–180.

Hammer, Ø., Harper, D. A. T. and Ryan, P. D. 2001. PAST: Paleontological Statistics Software Package for Education and Data Analysis. Palaeontologia Electronica, 4, 9 p.

Hanssen-Bauer, I. and Førland, E. J. 1998. Long-term trends in precipitation and temperature in the Norwegian Arctic: can they be explained by changes in atmospheric circulation patterns? Climate Research, 10, 143–153.

Heiri, O., Brooks, S. J., Birks, H. J. B. and Lotter, A. F. 2011. A 274-lake calibration data-set and inference model for chironomid-based summer air temperature reconstruction in Europe. Quaternary Science Reviews, 30, 3445–3456.

Heiri, O. and Lotter, A. F. 2001. Effect of low count sums on quantitative environmental reconstructions: an example using subfossil chironomids. Journal of Paleolimnology, 26, 343–350.

Heiri, O., Lotter, A. F. and Lemcke, G. 2001. Loss on ignition as a method for estimating organic and carbonate content in sediments: reproducibility and comparability of results. Journal of Paleolimnology, 25, 101–110.

Helama, S., Timonen, M., Holopainen, J., Ogurtsov, M. G., Mielikäinen, K., Eronen, M., Lindholm, M. and Meriläinen, J. 2009. Summer temperature variations in Lapland during the Medieval Warm Period and the Little Ice Age relative to natural instability of thermohaline circulation on multi-decadal and multi-centennial scales. Journal of Quaternary Science, 24, 450–456.

Hill, M. O. 1973. Diversity and Evenness: A Unifying Notation and Its Consequences. Ecology, 54, 427–432.

Hjelle, A. 1993. Geology of Svalbard, Norsk Polarinstitutt, Oslo. 162 p.

Hofmann, W. 1988. The significance of chironomid analysis (Insecta: Diptera) for paleolimnological research. Palaeogeography Palaeoclimatology Palaeoecology, 62, 501–509.

Holmgren, S. U., Bigler, C., Ingólfsson, Ó. and Wolfe, A. P. 2010. The Holocene–Anthropocene transition in lakes of western Spitsbergen, Svalbard (Norwegian High Arctic): climate change and nitrogen deposition. Journal of Paleolimnology, 43, 393–412.

Holtedahl, O. 1920. On the Paleozoic Series of Bear Island, especially on the Heclahook System. Norsk Geologisk Tidsskrift, 5, 121–148.

Horn, G. and Orvin, A. K. 1928. Geology of Bear Island. Skrifter om Svalbard og Ishavet 15, 152.

Hurrell, J. W. 1995. Decadal Trends in the North Atlantic Oscillation: Regional Temperatures and Precipitation. Science, 269, 676–679.

Hyvärinen, H. 1968. Late-Quaternary Sediment Cores from Lakes on Bjørnøya. Geografiska Annaler. Series A, Physical Geography, 50, 235–245.

Hyvärinen, H. 1970. Flandrian Pollen Diagrams from Svalbard. Geografiska Annaler. Series A, Physical Geography, 52, 213–222.

ISO 7724-2. Paints and varnishes — Colorimetry — Part 2: Colour measurement 1984. 6 p.

Izaguirre, I., Allende, L. and Marinone, M. C. 2003. Comparative study of the planktonic communities of three lakes of contrasting trophic status at Hope Bay (Antarctic Peninsula). Journal of Plankton Research, 25, 1079–1097.

Jónsdóttir, I. S., Augner, M., Fagerström, T., Persson, H. and Stenström, A. 2000. Genet age in marginal populations of two clonal Carex species in the Siberian Arctic. Ecography, 23, 402–412.

Jost, L. 2006. Entropy and diversity. Oikos, 113, 363–375.

Juggins, S. 2003. Software for ecological and palaeoecological data analysis and visualisation. User guide Version 1.5. , University of Newcastle, Newcastle. 73 p.

Kaufman, D. S., Schneider, D. P., McKay, N. P., Ammann, C. M., Bradley, R. S., Briffa, K. R., Miller, G. H., Otto-Bliesner, B. L., Overpeck, J. T., Vinther, B. M. and Arctic Lakes 2k Project Members. 2009. Recent Warming Reverses Long-Term Arctic Cooling. Science, 325, 1236–1239.

Klemetsen, A., Grotnes, P. E., Holthe, H. and Kristoffersen, K. 1985. Bear Island Charr. Report of Institute of Freswater Research Drottningholm, 62, 98–119.

Kreutz, K. J., Mayewski, P. A., Meeker, L. D., Twickler, M. S., Whitlow, S. I. and Pittalwala, I. I. 1997. Bipolar Changes in Atmospheric Circulation During the Little Ice Age. Science, 277, 1294–1296.

Kurek, J. and Cwynar, L. C. 2009. The potential of site-specific and local chironomid-based inference models for reconstructing past lake levels. Journal of Paleolimnology, 42, 37–50.

Landvik, J. Y., Bondevik, S., Elverhøi, A., Fkeldskaar, W., Mangerud, J., Salvigsen, O., Siegert, M. J., Svendsen, J.-I. and Vorren, T. O. 1998. The last glacial maximum of Svalbard and the Barents Sea area: Iice sheet extent and configuration. Quaternary Science Reviews, 17, 43–75.

Langdon, P. G., Ruiz, Z., Brodersen, K. P. and Foster, I. D. L. 2006. Assessing lake eutrophication using chironomids: understanding the nature of community response in different lake types. Freshwater Biology, 51, 526–577.

Luoto, T. P. 2011. The relationship between water quality and chironomid distribution in Finland—A new assemblage-based tool for assessments of long-term nutrient dynamics. Ecological Indicators, 11, 255–262.

Luoto, T. P. 2013. How cold was the Little Ice Age? A proxy-based reconstruction from Finland applying modern analogues of fossil midge assemblages. Environmental Earth Sciences, 68, 1321–1329.

Luoto, T. P., Brooks, S. J. and Salonen, V.-P. 2014a. Ecological responses to climate change in a bird-impacted High Arctic pond (Nordaustlandet, Svalbard). Journal of Paleolimnology, 51, 87–97.

Luoto, T. P., Nevalainen, L., Kubischta, F., Kultti, S., Knudsen, K. L. and Salonen, V.-P. 2011. Late Quaternary ecological turnover in High Arctic lake Einstaken, Nordaustlandet, Svalbard (80° N). Geografiska Annaler. Series A, Physical Geography, 93, 337–354.

Luoto, T. P., Oksman, M. and Ojala, A. E. K. 2014b. Climate change and bird impact as drivers of High Arctic pond deterioration. Polar Biology, in press. DOI: 10.1007/s00300-014-1592-9

Luterbacher, J., Xoplaki, E., Dietrich, D., Jones, P. D., Davies, T. D., Portis, D., Gonzalez-Rouco, J. F., Storch, H. v., Gyalistras, D., Casty, C. and Wanner, H. 2002. Extending North Atlantic Oscillation reconstructions back to 1500. Atmospheric Science Letters, 2, 114–124.

Mangerud, J. and Landvik, J. Y. 2007. Younger Dryas cirque glaciers in western Spitsbergen: smaller than during the Little Ice Age. Boreas, 36, 278–285.

Mann, M. E. and Jones, P. D. 2003. Global surface temperatures over the past two millennia. Geophysical Research Letters, 30, 1820–1824.

Masson-Delmotte, V., Schulz, M., Abe-Ouchi, A., Beer, J., Ganopolski, A., Rouco, J. F. G., Jansen, E., K. Lambeck, Luterbacher, J., Naish, T., Osborn, T., Otto-Bliesner, B., Quinn, T., Ramesh, R., Rojas, M., Shao, X. and Timmermann, A. 2013. Information from Paleoclimate Archives. In: Stocker, T. F., Qin, D., Plattner, G.-K., Tignor, M., Allen, S. K., Boschung, J., Nauels, A., Xia, Y., Bex, V. and Midgley, P. M. (eds.) Climate Change 2013: The Physical Science Basis. Contribution of Working Group I to the Fifth Assessment Report of the Intergovernmental Panel on Climate Change. Cambridge University Press. Cambridge.

Matthews, J. A. and Briffa, K. R. 2005. The 'Little Ice Age': re-evaluation of an evolving concept. Geografiska Annaler. Series A, Physical Geography, 87**,** 17–36.

McKay, N. P. and Kaufman, D. S. 2014. An extended Arctic proxy temperature database for the past 2,000 years. Scientific Data, 1:140026. DOI: 10.1038/sdata.2014.26

Michelutti, N., Blais, J. M., Liu, H., Keatley, B. E., M.S.V., D., Mallory, M. L. and Smol, J. P. 2008. A test of the possible influence of seabird activity on the 210Pb flux in high Arctic ponds at Cape Vera, Devon Island, Nunavut: implications for radiochronology. Journal of Paleolimnology, 40**,** 783–791.

Michelutti, N., Mallory, M. L., Blais, J. M., Douglas, M. S. V. and Smol, J. P. 2011. Chironomid assemblages from seabird-affected High Arctic ponds. Polar Biology, 34**,** 799–812.

Miettinen, A., Koç, N., Hall, I. R., Godtliebsen, F. and Divine, D. 2011. North Atlantic sea surface temperatures and their relation to the North Atlantic Oscillation during the last 230 years. Climate Dynamics, 36**,** 533–543.

Miller, G. H., Brigham-Grette, J., Alley, R. B., Anderson, L., Bauch, H. A., M.S.V., D., Edwards, M. E., Elias, S. A., Finney, B. P., Fitzpatrick, J. J., Funder, S. V., Herbert, T. D., Hinzman, L. D., Kaufman, D. S., MacDonald, G. M., Polyak, L., Robock, A., Serreze, M. C., Smol, J. P., Spielhagen, R., White, J. W. C., Wolfe, A. P. and Wolff, E. W. 2010. Temperature and precipitation history of the Arctic. Quaternary Science Reviews, 29**,** 1679–1715.

Moberg, A., Sonechikin, D. M., Holmgren, K., Datsenko, N. M. and Karlén, W. 2005. Highly variable Northern Hemisphere temperatures reconstructed from low- and high-resolution proxy data. Nature, 433**,** 613–617.

Nansen, F. 1922. The strandflat and isostasy. Videnskapsselskapets Skrifter 1, 11**,** 1–313.

Nathorst, A. G. 1899. Några upplysningar till den nya kartan öfver Beeren Eiland. Ymer, 19**,** 171–185.

Nesje, A. 1992. A Piston Corer for Lacustrine and Marine Sediments. Arctic and Alpine Research, 24**,** 257–259.

Nesje, A. and Dahl, S. O. 2001. The Greenland 8200 cal. yr BP event detected in loss-on-ignition profiles in Norwegian lacustrine sediment sequences. Journal of Quaternary Science, 16**,** 155–166.

Nordli, P. Ø., Hanssen-Bauer, I. and Førland, E. J. 1996. Homogenity analyses of temperature and precipitation series from Svalbard and Jan Mayen. DNMI-Report 16/96 KLIMA.Norwegian Meteorological Institute. 41 p.

Norwegian Polar Institute.1992. Topopgraphical map of Svalbard S100, sheet D20 Bjørnøya, 1 :50 000. Oslo.

Oldfield, F., Barnosky, C., Leopold, E. B. and Smith, J. P. 1983. Mineral magnetic studies of lake sediments. Hydrobiologia, 103**,** 37–44.

Oldfield, F., Crooks, P. R. J., Harkness, D. D. and Petterson, G. 1997. AMS radiocarbon dating of organic fractions from varved lake sediments: an empirical test of reliability. Journal of Paleolimnology, 18**,** 87–91.

Olsen, J., Anderson, N. J. and Knudsen, M. F. 2012. Variability of the North Atlantic Oscillation over the past 5,200 years. Nature Geoscience, 5**,** 808–812.

Oswald, W. W., Andrerson, P. M., Brown, T. A., Brubaker, L. B., Hu, F. S., Lozhkin, A. V., Tinner, W. and Kaltenrieder, P. 2005. Effects of sample mass and macrofossil type on radiocarbon dating of arctic and boreal lake sediments. The Holocene, 15**,** 758–767.

Overpeck, J. T., Hughen, K., Hardy, D., Bradley, R. S., Case, R., Douglas, M., Finney, B., Gajewski, K., Jacoby, G., Jennings, A., Lamoureux, S. F., Lasca, A., MacDonald, G. M., Moore, J., Retelle, M., Smith, S., Wolfe, A. P. and Zielinski, G. 1997. Arctic Environmental Change of the Last Four Centuries. Science, 278**,** 1251–1256.

Pages 2k Consortium. 2013. Continental-scale temperature variability during the past two millennia. Nature Geoscience, 6, 339–346.

Quinlan, R., Douglas, M. S. V. and Smol, J. P. 2005. Food web changes in arctic ecosystems related to climate warming. Global Change Biology, 11, 1381–1386.

Quinlan, R. and Smol, J. P. 2001a. Chironomid-based inference models for estimating end-of-summer hypolimnetic oxygen from south-central Ontario shield lakes. Freshwater Biology, 46, 1529–1551.

Quinlan, R. and Smol, J. P. 2001b. Setting minimum head capsule abundance and taxa deletion criteria in chironomid-based inference models. Journal of Paleolimnology, 26, 327–342.

Salonen, V.-P., Eronen, M. and Saarnisto, M. 2002. Käytännön maaperägeologia. 2nd edition, Kirja-Aurora, Turku. 237 p.

Salvigsen, O. and Slettemark, Ø. 1995. Past glaciation and sea levels on Bjørnøya, Svalbard. Polar Research, 14, 245–251.

Sandgren, P. and Snowball, I. 2001. Application of mineral magnetic techniques to paleolimnology. In: Last, W. M. and Smol, J. P. (eds.) Tracking Environmental Change Using Lake Sediments. Volume 2: Physical and Chemical Techniques. Kluwer Academic Puplishers. Dordrecht, The Netherlands. 217–237.

Self, A. E., Brooks, S. J., Birks, H. J. B., Nazarova, L., Porinchu, D., Odland, A., Yang, H. and Jones, V. J. 2011. The distribution and abundance of chironomids in high-latitude Eurasian lakes with respect to temperature and continentality: development and application of new chironomid-based climate-inference models in northern Russia. Quaternary Science Reviews, 30, 1122–1141.

Serreze, M. C. and Francis, J. A. 2006. The Arctic amplification debate. Climatic Change, 76, 241–264.

Spielhagen, R., Werner, K., Sørensen, S. A., Zamelczyk, K., Kandiano, E., Budeus, G., Husum, K., Marchitto, T. M. and Hald, M. 2011. Enhanced Modern Heat Transfer to the Arctic by Warm Atlantic Water. Science, 331, 450–453.

Stahl, J. B. 1969. The uses of chironomids and other midges in interpreting lake histories. Mitteilungen lnternationale Vereinigung für Theoretische und Angewandte Limnologie, 17, 111–125.

Svendsen, J.-I. and Mangerud, J. 1997. Holocene glacial and climatic variations on Spitsbergen, Svalbard. The Holocene, 7, 45–57.

Thompson, R., Battarbee, R. W., O'Sullivan, P. E. and Oldfield, F. 1975. Magnetic Susceptibility of Lake Sediments. Limnology and Oceanography, 20, 687–698.

Trouet, V., Esper, J., Graham, N. E., Baker, A., Scourse, J. D. and Frank, D. C. 2009. Persistent Positive North Atlantic Oscillation Mode Dominated the Medieval Climate Anomaly. Science, 324, 78–80.

Tuomisto, H. 2010. A consistent terminology for quantifying species diversity? Yes, it does exist. Oecologia, 164, 853–860.

Turner, J. and Marshall, G. J. 2011. Climate Change in the Polar Regions, Cambridge University Press, Cambridge. 434 p.

Velle, G., Kongshavn, K. and Birks, H. J. B. 2011. Minimizing the edge-effect in environmental reconstructions by trimming the calibration set: Chironomid-inferred temperatures from Spitsbergen. The Holocene, 21, 417–430.

Vinje, T. 1998. On the variation during the past 400 years of the Barents Sea ice edge position and Northern Hemisphere temperatures. Proceedings of the WCRP Symposium on Polar Processes and Global Climate, Rosario, Orcas Island, WA, USA. p. 271–273.

Vinje, T. 2001. Anomalies and Trends of Sea-Ice Extent and Atmospheric Circulation in the Nordic Seas during the Period 1864–1998. Journal of Climate, 14, 255–267.

Visbeck, M., Chassignet, E. P., Curry, R., Delworth, T., Dickson, B. and Krahmann, G. 2003. The Ocean's Response to North Atlantic Oscillation Variability. In: Hurrell, J. W., Kushnir, Y., Ottersen, G. and Visbeck, M. (eds.) The North Atlantic Oscillation: Climatic Significance and Environmental Impact. American Geophysical Union. Washington D. C., 113–146.

Walker, I. R. 2001. Midges: Chironomidae and related Diptera. In: Smol, J. P., Birks, H. J. B. and Last, W. M. (eds.) Tracking environmental change using lake sediments. Volume 4: Zoological indicators. Kluwer Academic Publishers. Dordrecht, The Netherlands. 43–66.

Walker, I. R. and Cwynar, L. C. 2006. Midges and palaeotemperature reconstruction—the North American experience. Quaternary Science Reviews, 25, 1911–1925.

Walker, I. R., Smol, J. P., Engstrom, D. R. and Birks, H. J. B. 1991. An assessment of Chironomidae as quantitative indicators of past climatic change. Canadian Journal of Fisheries and Aquatic Sciences, 48, 975–987.

Wanner, H., Solomina, O., Grosjean, M., Ritz, S. P. and Jetel, M. 2011. Structure and origin of Holocene cold events. Quaternary Science Reviews, 30, 3109–3123.

Willemse, N. W. and Törnqvist, T. E. 1999. Holocene century-scale temperature variability from West Greenland lake records. Geology, 27, 580–584.

Wohlfarth, B., Lemdahl, G., Olsson, S., Persson, T., Snowball, I., Ising, J. and Jones, V. 1995. Early Holocene environment on Bjørnøya (Svalbard) inferred from multidisciplinary lake sediment studies. Polar Research, 14, 253–275.

Wolfe, A. P., Miller, G. H., Olsen, C. A., Forman, S. L., Doran, P. T. and Holmgren, S. U. 2004. Geochronology of high latitude lake sediments. In: Pienitz, R., Douglas, M. S. V. and Smol, J. P. (eds.) Long-term Environmental Change in Arctic and Antarctic Lakes. Developments in Paleoenvironmental Research: Volume 8. Kluwer Academic Publishers. Dordrecht, The Netherlands. 19–52.

Wolfe, A. P., Vinebrooke, R. D., Michelutti, N., Rivard, B. and Das, B. 2006. Experimental calibration of lake-sediment spectral reflectance to chlorophyll a concentrations: methodology and paleolimnological validation. Journal of Paleolimnology, 36, 91–100.

Worsley, D., Agdestein, T., Gjelberg, J. G., Kirkemo, K., Mørk, A., Nilsson, I., Olaussen, S., Steel, R. J. and Stemmerik, L. 2001. The geological evolution of Bjørnøya, Arctic Norway: implications for the Barents Shelf. Norsk Geologisk Tidsskrift, 81, 195–234.

Worsley, D. and Edwards, M. B. 1976. The Upper Palaeozoic succession of Bjørnøya. Norsk Polarinstitutt Årbok 1974, 17–34.

Appendix 1. ^{210}Pb dating results from the surface sediments of lake Ellasjøen

A. Fallout radionuclide concentrations in the lake Ellasjøen sediment core ESGC1-13

Depth		^{210}Pb Total		^{210}Pb Unsupported		^{210}Pb Supported		^{137}Cs	
cm	g cm^{-2}	Bq kg^{-1}	±	Bq kg^{-1}	±	Bq kg^{-1}	±	Bq kg^{-1}	±
0.25	0.01	724.7	28.0	631.3	28.5	93.4	5.5	89.9	5.0
1.25	0.11	785.1	31.0	698.7	31.6	86.4	5.9	111.6	5.4
2.25	0.23	868.0	29.3	780.6	29.7	87.4	4.8	137.0	6.1
3.25	0.31	811.9	45.9	735.2	46.5	76.7	7.6	141.3	8.6
4.25	0.53	839.2	47.1	748.8	47.7	90.4	7.6	229.6	11.4
6.25	0.76	549.6	23.2	478.4	23.6	71.2	4.0	317.0	6.7
8.25	0.99	501.9	20.7	420.5	21.1	81.5	3.8	241.9	6.2
11.25	1.37	263.0	18.6	174.9	19.3	88.2	5.0	292.8	6.3
14.25	1.90	161.2	18.2	58.7	18.6	102.6	3.9	8.6	2.5
17.25	2.49	92.9	11.1	20.2	11.5	72.7	3.0	0.0	0.0
19.75	3.01	74.8	10.6	-1.3	10.9	76.1	2.6	1.6	1.4

B. ^{210}Pb chronology of the lake Ellasjøen sediment core ESGC1-13

Depth		Chronology Date	Age		Sedimentation Rate		
cm	g cm^{-2}	AD	y	±	g cm^{-2} y^{-1}	cm y^{-1}	± (%)
0.00	0.00	2013	0	0			
0.25	0.01	2013	0	1	0.042	0.50	5.6
1.25	0.11	2010	3	2	0.037	0.34	5.7
2.25	0.23	2007	6	2	0.033	0.31	5.5
3.25	0.31	2004	9	2	0.027	0.18	7.6
4.25	0.53	1996	17	3	0.025	0.17	8.0
6.25	0.76	1986	27	4	0.024	0.21	8.1
8.25	0.99	1977	36	5	0.026	0.21	10.3
11.25	1.37	1963	50	9	0.014	0.12	9.3
14.25	1.90	1926	87	10	0.014	0.08	9.3
17.25	2.49	1883	130	12	0.014	0.07	9.3

C. Suggested CRS age-depth model with assumed recent high sedimentation rate

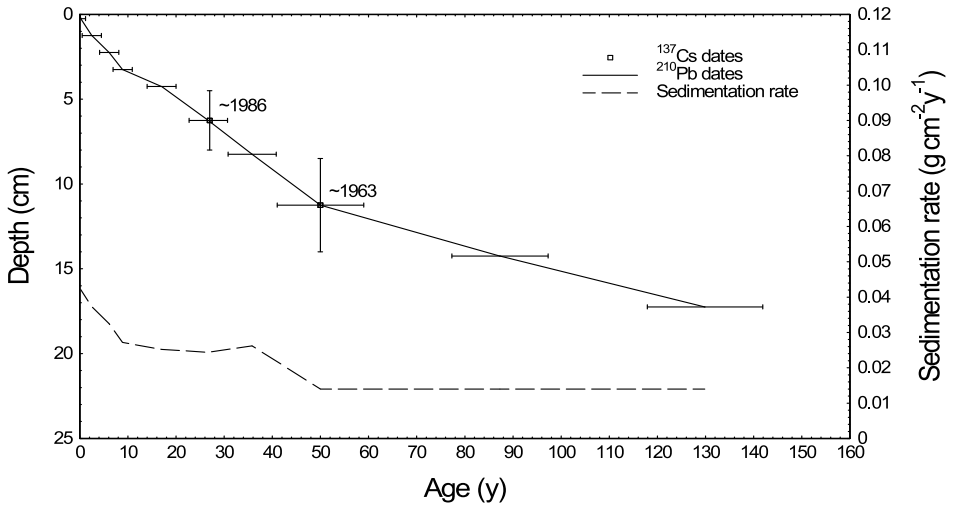

Appendix 2. Photographs of chironomid headcapsules from Ellasjøen. A) *Microspectra contracta*-type, B) *Microspectra radialis*-type, C) *Paratanytarsus austriacus*-type, D) *Heterotrissocladius maeaeri*-type, E) *Cricotopus type P*-type, F) *Heterotrissocladius grimshawi*-type and G) *Orthocladius type S*-type. Mentum structures and other features can be seen to vary from speciestype to another in well preserved remains.